LCGC™ INTERNATIONAL

VOL. 1 NO. 1 | JANUARY 2024

AN MH life sciences BRAND

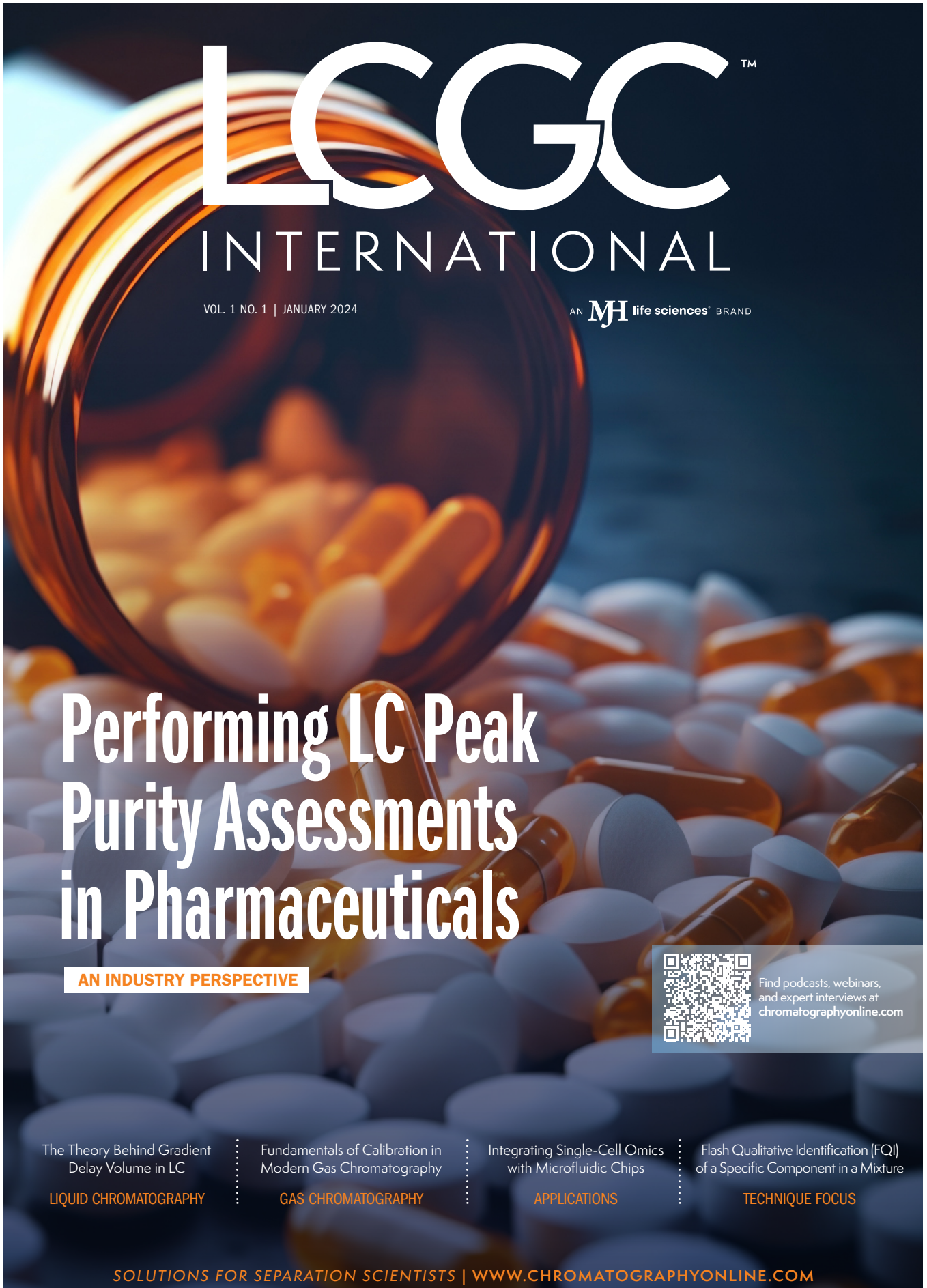

LCGC™ INTERNATIONAL

VOL. 1 NO. 1 | JANUARY 2024

AN MJH life sciences® BRAND

Performing LC Peak Purity Assessments in Pharmaceuticals

AN INDUSTRY PERSPECTIVE

Find podcasts, webinars, and expert interviews at **chromatographyonline.com**

The Theory Behind Gradient Delay Volume in LC
LIQUID CHROMATOGRAPHY

Fundamentals of Calibration in Modern Gas Chromatography
GAS CHROMATOGRAPHY

Integrating Single-Cell Omics with Microfluidic Chips
APPLICATIONS

Flash Qualitative Identification (FQI) of a Specific Component in a Mixture
TECHNIQUE FOCUS

Paradigm Shift in GCxGC Workflows: Unlocking the Potential of Complex Sample Characterization

LECO's Paradigm Reverse Fill-Flush (RFF) Modulator

- Cryogen-free modulation featuring backpressure-controlled loop filling improves ease-of-use and method development for Reverse Fill-Flush GCxGC
- Accessible and Efficient: Say Goodbye to Finicky Modulator Design with Standard Wrench-Friendly Column and Loop Fittings

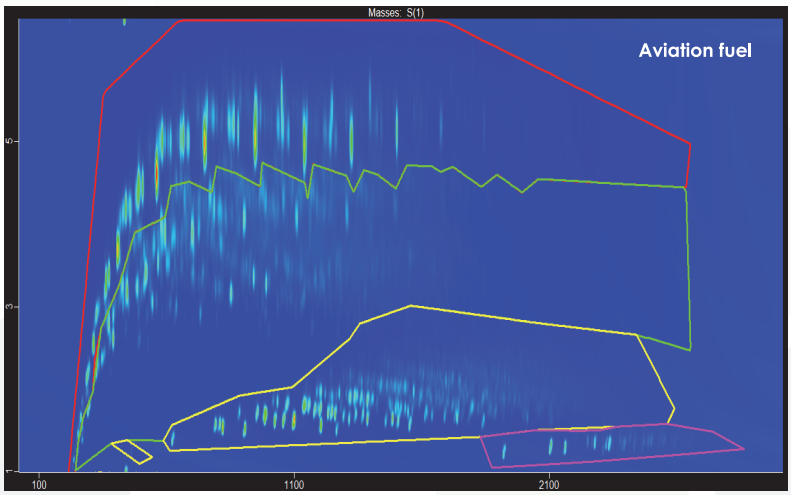

Shift Flow Splitter

- Maintains a Consistent Split Ratio between MS and FID, even during the GC oven ramp
- Easily paired with the Paradigm flow modulator thanks to high flow rate handling (approximately 20 mL/min) for simultaneous TOF / FID acquisition

Visit https://www.leco.com/product/reverse-flow-modulator

Phone: 1-800-292-6141 | info@leco.com
www.leco.com | © 2024 LECO Corporation

LECO
EMPOWERING RESULTS
Elemental Analysis | GC Mass Spectrometry | Metallography

CONTENTS

JANUARY 2024 | VOLUME 1 | NO. 1

COVER STORY

COLUMNS

ON THE COVER

Performing chromatographic peak purity assessments (PPA) in the pharmaceutical industry.

Vladimir Polikarpov (Generated with AI)

ARTICLE

SPECIAL SECTION

DEPARTMENTS

LCGC International™ (ISSN 1527-5949 print) (ISSN 1939-1889 digital) is published monthly by MultiMedia Healthcare, LLC., 2 Commerce Drive Cranbury, NJ 08512, and is distributed free of charge to users and specifiers of chromatographic equipment in the United States and Canada. LCGC is available on a paid subscription basis to nonqualified readers in the United States and its possessions at the rate of: 1 year (13 issues), $106.00; in Canada and Mexico: 1 year (13 issues), $135.00; in all other countries: 1 year (13 issues), $212.00. Periodicals postage paid at Trenton, NJ 08650 and additional mailing offices. POSTMASTER: Please send address changes to LCGC, P.O. Box 457, Cranbury NJ 08512-0457. PUBLICATIONS MAIL AGREEMENT NO. 40612608, Return Undeliverable Canadian Addresses to: IMEX Global Solutions, P. O. Box 25542, London, ON N6C 6B2, CANADA Canadian GST number: R-124213133RT001. Printed in the USA.

LCGC INTERNATIONAL

AN MJH life sciences BRAND

485F US Highway One South, Suite 210
Iselin, NJ 08830 | (609) 716-7777

Founder
Mike Hennessy Sr | 1960 - 2021

EAB Members

INTERESTED IN JOINING THE EDITORIAL BOARD?

Contact **John Chasse, jchasse@mjhlifesciences.com** for more information on how to get involved with the LCGC International Editorial Advisory Board.

Subscribe for more content
get practical tips and valuable resources

MANUSCRIPTS: For manuscript preparation guidelines, see chromatographyonline.com/lcgc-author-guidelines, or call The Editor, (609) 716-7777. LCGC welcomes unsolicited articles, manuscripts, photographs, illustrations, and other materials but cannot be held responsible for their safekeeping or return. Every precaution is taken to ensure accuracy, but LCGC cannot accept responsibility for the accuracy of information supplied herein or for any opinion expressed.

SUBSCRIPTIONS: For subscription and circulation information: LCGC, P.O. Box 457, Cranbury, NJ 08512-0457, or email mmhinfo@mmhgroup.com. Delivery of LCGC outside the United States is 14 days after printing. (LCGC Europe and LCGC Asia Pacific are available free of charge to users and specifiers of chromatographic equipment in Western Europe and Asia and Australia, respectively.)

CHANGE OF ADDRESS: Send change of address to LCGC, P.O. Box 457, Cranbury, NJ 08512-0457; alternately, send change via e-mail to mmhinfo@mmhgroup.com. Allow four to six weeks for change. PUBLICATIONS MAIL AGREEMENT No. 40612608. Return all undeliverable Canadian addresses to: IMEX Global Solutions, P.O. Box 25542, London, ON, N6C 6B2, CANADA. Canadian GST number: R-124213133RT001.

C.A.S.T. DATA AND LIST INFORMATION: Contact Stephanie Shaffer, tel. (774) 249-1890, e-mail: SShaffer@mjhlifesciences.com.

INTERNATIONAL LICENSING: Contact Kim Scaffidi, e-mail: kscaffidi@mjhassoc.com

CUSTOMER INQUIRIES: Customer inquiries can be forwarded directly to MJH Life Sciences, Attn: Subscriptions, 2 Clarke Drive, Suite 100, Cranbury, NJ 08512; e-mail: mmhinfo@mmhgroup.com

OPTIMIZE YOUR INSTRUMENTATION FOR HIGH SPEED, HIGH THROUGHPUT

MICRO AND NANO FLOW UHPLC

Cheminert UHPLC injectors, switching valves, and selectors make it easy. Internal volume is minimized with zero dead volume. A proprietary rotor material and stator coating on some models achieve pressures up to 20,000 psi,suitable for the most demanding analytical techniques. All models are compatible with any VICI actuation option.

FEATURES

- UHPLC applications
- Pressures available in 10k, 15k, and 20k psi
- Bore sizes from 100-250 µm
- Fitting sizes available in 360 µm to 1/16”
- Zero dead volume

VICI
www.vici.com
(800) 367-8424
sales_usa@vici.com

ONLINE HIGHLIGHTS

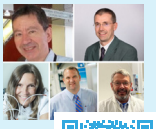

ChromSoc Announces 2024 Martin and Silver Jubilee Medal Winners

The Chromatographic Society will honor five scientists and academics next year, conferring its highest honor, the Martin Medal, to David McCalley and Fabrice Gritti.

SCAN QR CODE FOR LINK

PFAS in Aquatic Environments: An Interview with Yuefei Ruan from the City University of Hong Kong

Ruan discusses her team's research on the importance of monitoring PFAS in aquatic environments.

SCAN QR CODE FOR LINK

***LCGC International* 2024 New Product Review – Call For Submissions**

You're invited to publicize your 2023–2024 new product introductions in *LCGC International*.

SCAN QR CODE FOR LINK

CONNECT WITH LCGC

Teaching it Forward in Separation Science

Co-hosts Dwight Stoll and James Grinias talk with Kevin Schug, Shimadzu Distinguished Professor of Analytical Chemistry at the University of Texas, Arlington.

SCAN QR CODE FOR LINK

'Like' our page LCGC

Follow us @ LC_GC

Join the LCGC LinkedIn group

NOTE FROM THE CEO

WE ARE THRILLED to bring you the first issue of *LCGC International* for January 2024, marking the beginning of an exciting year in chromatography. This inaugural issue is a treasure trove of insights, focusing on pharmaceuticals and biopharmaceuticals, and delving deep into the realms of liquid and gas chromatography. Within these pages, you'll find columns written by experts who are passionate about sharing their knowledge.

Dwight R. Stoll unravels the mysteries surrounding the gradient delay volume in his "LC Troubleshooting" column. This often-overlooked parameter plays a crucial role in gradient elution separations, impacting both method development and the quality of separation. Stoll not only explores its physical connection to LC instruments, but also shares best practices for developing methods that seamlessly transition between instruments.

In "GC Connections," Nicholas H. Snow asks "How Big Are Your Peaks? Fundamentals of Calibration in Gas Chromatography." As gas chromatographs become more user-friendly, and data systems more powerful, Snow sheds light on the fundamentals of calibration, comparing and contrasting different methods, and offering recommendations for tackling quantitative challenges.

"Focus on Biopharmaceutical Analysis" shines a spotlight on emerging trends and technologies pertaining to the integration of single-cell omics with microfluidic chips. This piece explores the revolutionary impact of these techniques in understanding cellular heterogeneity, and their role in complementing genomics and transcriptomics studies.

Our two peer-reviewed articles add a layer of scientific depth to this issue. In our cover story, "Liquid Chromatographic Peak Purity Assessments in Forced Degradation Studies: An Industry Perspective," Pascal Marillier and his co-authors provide a comprehensive overview of scientific rationales and best practices in the pharmaceutical industry. The focus is on chromatographic peak purity assessments (PPAs) and their crucial role in the development and validation of stability-indicating analytical methods.

Finally, from Henan Polytechnic University and Pingdingshan University in China, a team led by Lizhi Cui introduces a groundbreaking flash qualitative identification method within their peer-reviewed article. This method, based on a diode array detector (DAD), promises a fast, alternative method to qualitatively identify specific components within mixtures.

As you explore the pages of this issue, you'll find a rich tapestry of knowledge and innovation. I invite you to immerse yourself in the diverse topics presented by our expert contributors. On behalf of the entire editorial team, we hope this issue sparks inspiration and furthers your understanding of the dynamic world of chromatography.

Happy reading, and Happy New Year! ■

Mike Hennessy, Jr.
President & CEO, MJH Life Sciences®

LCGC is a multimedia platform that helps chromatographers keep up to date with the latest trends and developments in separation science, and supports them to perform more effectively in the workplace. Keep updated with our multimedia content by visiting the global website (www.chromatographyonline.com), subscribing to our newsletters, and attending our wide range of educational virtual symposiums and webinars.

HAMILTON

Build Your Own HPLC Column

Hamilton offers 21 polymer-based stationary phases and two silica gels (C8 and C18) to satisfy most separation/purification needs. Our specialty resins are offered in a wide variety of hardware dimensions.

Hamilton gives you control to build any column to your specifications with any of our stationary phases in any combination of our column hardware formats.

NEED HELP DECIDING WHICH HPLC COLUMN IS RIGHT FOR YOU?

It's simple! Follow these three steps:

Choose Your Stationary Phase

If you need additional information to determine which chemistry fits your application needs, check out our application index with over 1,700 compounds separated at hamiltoncompany.com/hplc. Hamilton Company specializes in polymer stationary phases and offers silica stationary phases covering reversed-phase, anion exchange, cation exchange, and ion exclusion separation mechanisms, including many USP "L" methodologies.

Select the Particle Size and Hardware Dimensions

We Build It!

For more information, visit **www.hamiltoncompany.com/build-your-own-hplc-column**

HAMILTON

Web: **www.hamiltoncompany.com**
USA: **800-648-5950**
Europe: **+41-58-610-10-10**

Hamilton Americas & Pacific Rim
Hamilton Company Inc.
4970 Energy Way
Reno, Nevada 89502 USA
Tel: +1-775-858-3000
Fax: +1-775-856-7259
sales@hamiltoncompany.com

Hamilton Europe, Asia & Africa
Hamilton Bonaduz A.G.
Via Crusch 8
CH-7402 Bonaduz, Switzerland
Tel: +41-58-610-10-10
contact.pa.ch@hamilton.ch

The Gradient Delay Volume, Part I: Theory

Dwight R. Stoll

The gradient delay volume is arguably one of the most important, yet least appreciated, parameters affecting how gradient elution separations in LC work. This has implications both for method development and for method transfer during the life cycle of a LC method. In this installment, I will review the concept of gradient delay volume, its physical connection to the LC instrument, and how it can impact method development and separation quality.

IN MY INTERACTIONS with people learning about various aspects of LC, I find that the concept of "gradient delay volume" (GDV) is one of the most difficult ideas to grasp and apply in practice. I find this to be the case both for true beginners—students who are just learning the basics of LC—and for more experienced scientists who have always dealt with GDV, knowingly or unknowingly, but are perhaps having to think about its impacts on their work in new ways. The GDV concept has been important since the very first times LC separations involving changes in mobile phase composition were made during an analysis, an approach now known as "gradient elution" separations. However, given the various ways that GDV can impact the practice of LC, and that we continue to see changes in commercial instrumentation that affect the way we interact and think about GDV, I think a dive into the details is warranted here. In this installment of "LC Troubleshooting," I will review the basic elements of the GDV concept and discuss how we understand that GDV affects characteristics of LC separations from a theoretical point of view. In a subsequent installment, I will discuss the practical implications of these ideas.

A short list of the ways in which the GDV can impact LC separations includes the following:

- Adjusting the GDV, either physically or effectively, through software control, can be used as a variable when optimizing gradient elution separations.
- GDV can be an important parameter affecting the throughput of very fast LC separations.
- Differences between the GDVs of different LC instruments can lead to problems when transferring a method developed on one instrument to a different instrument.

The "gradient delay volume" is commonly referred to by others as the "gradient dwell volume," or sometimes just "dwell volume." I prefer the inclusion of "gradient" to make it clear what we are talking about, and I prefer "delay" over "dwell" because "delay" communicates one of the most important impacts of GDV—that it delays the arrival of a programmed change in mobile phase composition at the column inlet. Nevertheless, from my point of view, "gradient delay volume" and "gradient dwell volume" refer to the same thing.

In this two-part series on GDV, I will discuss details in a way that assumes we are talking about the reversed-phase mode of LC. However, most of the ideas that will be discussed are applicable, at least conceptually, to other modes of LC separation, such as HILIC and ion-exchange.

Finally, readers interested in learning more about GDV will not have a hard time finding good resources and are encouraged to consult them. A short list includes several articles in *LCGC* magazine and the book by Snyder and Dolan, which is focused entirely on gradient elution LC (1). Searching the LC Troubleshooting Bible website (https://lctsbible.com/) for the keyword "dwell volume" will immediately return about a dozen articles from the last 20 years.

What is Gradient Delay Volume?

By definition, gradient delay volume is the physical volume that occupies the fluidic path between the point at which two or more solvents are mixed in a LC pump (labeled the "convergence point" in Figure 1) and the column inlet. Figure 1 shows simplified schematic diagrams for the two designs of LC pumps in common

use today, which we refer to here as high-pressure mixing and low-pressure mixing designs (see reference [2] for an excellent review of pump designs, as well as a highly educational history of their development). In the case of the high-pressure mixing design shown in Figure 1a, two solvent streams metered by individual high-pressure pumps are brought together at the convergence point, and the combined stream only has to travel through a small mixer and connecting capillaries (and, importantly, the autosampler), before reaching the LC column. In the case of the low-pressure mixing design, the combined solvent flowing out of the convergence point first travels through the high-pressure pump head before moving on to the mixer, sampler, and the column. Typical gradient delay volumes associated only with the pump components (including mixer) are on the order of 50 and 400 µL for modern high- and low-pressure mixing designs, respectively. The gradient delay volumes associated with older models of low-pressure mixing designs were on the order of 1,000 µL. The injector/sampler component of the system can add a little (for example, with low-volume fixed loop injectors) or a lot (for example, with flow through needle designs) of delay volume depending on the design. For example, the additional volume could be on the order of a few microliters for low-volume fixed loop injectors, or as much as a few hundred microliters for a flow through needle design (3).

The difference between the mobile phase that we instruct the pump to deliver to the column as part of a gradient elution method, and what is actually delivered to the column, is illustrated in Figure 2. Here, we see that the initial onset of the actual change in mobile phase composition arriving at the column inlet is offset from what we instruct the pump to do by the gradient delay time, t_d (V_d/F). Then, following completion of the programmed gradient, we see that it takes some time for the strong solvent to be flushed out of the pump components before the actual composition of the mobile phase arriving at the column inlet returns to the composition that will be used as the starting point in the gradient applied in the next analysis. The time required for this flush-out is on the order of $2 \times t_d$.

When and Why is the Gradient Delay Volume Important?

Effect on Retention and Selectivity

When using gradient elution conditions, it is intuitively evident that any increase in the gradient delay volume will lead to an increase in retention time, simply because it will take longer for the onset of the change in mobile phase composition to reach the column, and thus it will take longer for the composition that actually elutes the compound to reach the column. We can quantify this effect by examining the relationship between retention time and GDV in a preferred retention equation that applies to gradient elution conditions. In the interest of simplicity, we'll look at the retention equation that comes from linear solvent strength (LSS) theory for reversed-phase LC (1). LSS asserts that the relationship between the

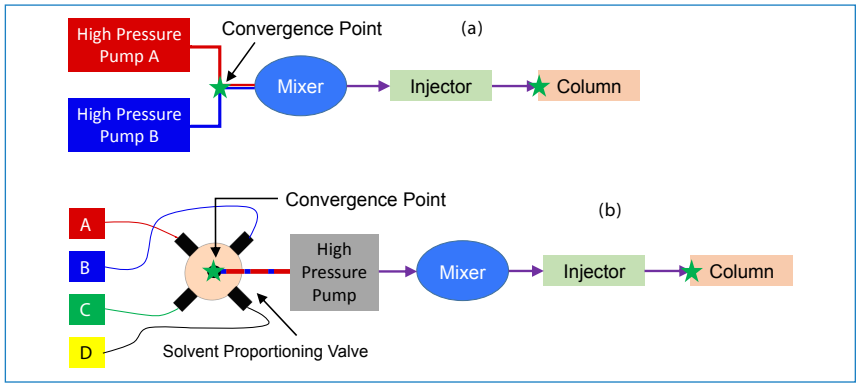

FIGURE 1: Simple schematics illustrating the differences between (a) high- and (b) low-pressure mixing designs used in LC pumps. The volumes of all components lying between the green stars contribute to the gradient delay volume.

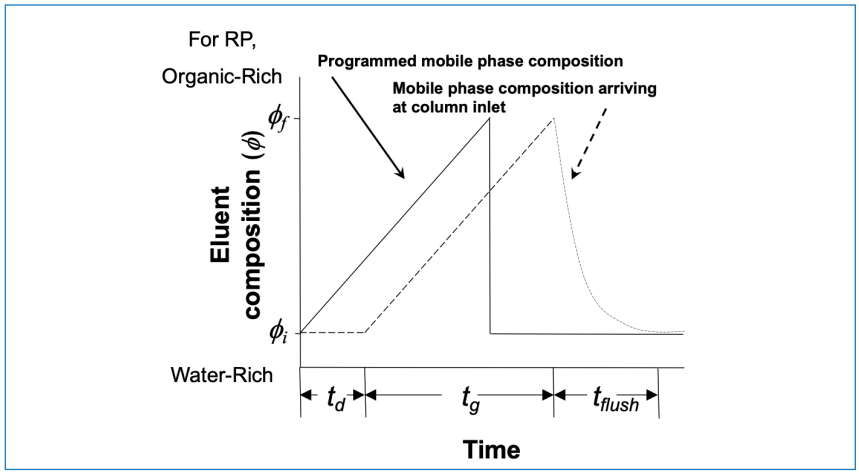

FIGURE 2: Solvent program used in gradient elution (solid line), and the mobile phase composition observed at the column inlet (dashed line). The change in composition is offset in time due to the delay time (t_d) that results from the time it takes for a change in composition to travel from the solvent convergence point in the pump to the column inlet. Reprinted from reference (4).

logarithm of retention factor and mobile phase composition (ϕ, on a 0–1 scale, where 0 represents pure weak solvent, and 1 represents pure strong solvent) is linear, as shown in equation 1, where $\ln(k_w)$ is the *y*-intercept of a plot of $\ln(k)$ vs. ϕ, and $-S$ is the slope (see Figure 6 for examples of this type of plot).

$$\ln(k) = \ln(k_w) - S \cdot \phi \quad [1]$$

In this case, a derivation involving an integration of the distance travelled by the analyte through the column with respect to time yields equation 2, which relates the retention time of the analyte (t_r) to $\ln(k_w)$ and S, the column dead volume (V_m), the mobile phase composition used as the starting point in the gradient (ϕ_i), the change in mobile phase composition during the gradient ($\Delta\phi$), the GDV (V_d), and the flow rate (F) (5). The parameter b is known as the gradient slope, given by equation 3, where t_g is the gradient time. Finally, k_i is the retention factor of the analyte in the mobile phase used as the starting point in the gradient (that is, ϕ_i). It is important to note that equation 2 only applies when $k_i \geq \frac{V_d}{V_m}$ and $t_r \leq t_g + t_d + t_m$—in other words, equation 2 only applies when the analyte elutes during the period when the mobile phase arriving at the column inlet is actually changing with respect to time.

$$t_r = \frac{V_m}{F} + \frac{V_d}{F} + \frac{V_m}{b \cdot F} \cdot \ln\left[b \cdot \left(k_i - \frac{V_d}{V_m}\right) + 1\right] \quad [2]$$

$$b = \frac{S \cdot \Delta\phi \cdot V_m}{F \cdot t_g} \quad [3]$$

Looking at equations 2 and 3, we see that the dependence of the retention time and the GDV is complex, because V_d appears both outside and inside the log term. When the retention of an analyte is low in the mobile phase used as the starting point in the gradient (ϕi), and as k_i approaches V_d/V_m, the influence of V_d on t_r decreases. On the other hand, for compounds that are strongly retained and elute late in the gradient (that is, k_i is large), then any change in V_d directly affects t_r. For example, if V_d is 100 µL and the flow rate is 400 µL/min, then increasing V_d to 500 µL will increase the retention times of all compounds eluting late in the gradient by 1 min.

Now, the fact that the influence of V_d on retention time varies depending on where a compound elutes with respect to the gradient time, and the fact that S and $\ln(k_w)$ influence retention time, means that there is the potential for V_d to influence not only retention time, but also selectivity. By using "selectivity" here, I mean that there is the potential for V_d to influence relative retention, and thus also resolution. The web-based HPLC simulator developed and maintained by my group (www.multidlc.org/hplcsim) is very useful for examining this type of phenomenon. The simulator is pre-loaded with retention parameters (which are calculated using LSS theory) that come from experimental measurements of retention time under reversed-phase conditions for about 40 small molecules, and we can simulate separations of these compounds while varying parameters such as flow rate, column dimensions, and GDV. Figure 3 shows the dependence of retention time on GDV for seven molecules. We see that in general retention increases with increasing GDV, as expected. However, the interesting thing is that some of the lines cross over each other, which is a result

of the fact that different compounds have different sensitivities to changes in mobile phase composition, as measured by the *S* parameter in equation 1. Now, the practical consequence of this, of course, is that wherever two or more of the lines intersect, there will be coelution of the compounds corresponding to those lines. This is illustrated in Figure 4, which shows the simulated chromatograms that we would expect for systems with GDV values of 200, 360, or 600 µL. With GDV values of 200 or 600 µL, there is serious overlap of the peaks for 3-phenylpropanol and methylparaben or methylparaben and benzonitrile, and the three compounds in that region of the chromatogram are not resolved. At 360 µL, however, all three compounds are resolved with a minimum resolution of about 1.5. This illustration shows that the impact of the GDV on separation selectivity can be both a blessing and a curse. On one hand, this phenomenon can be leveraged during method development as a means of optimizing a separation. On the other hand, if we are simply trying to transfer an already-developed method from one instrument to another, this phenomenon could lead to complications during the transfer if the GDVs for the two systems are not the same.

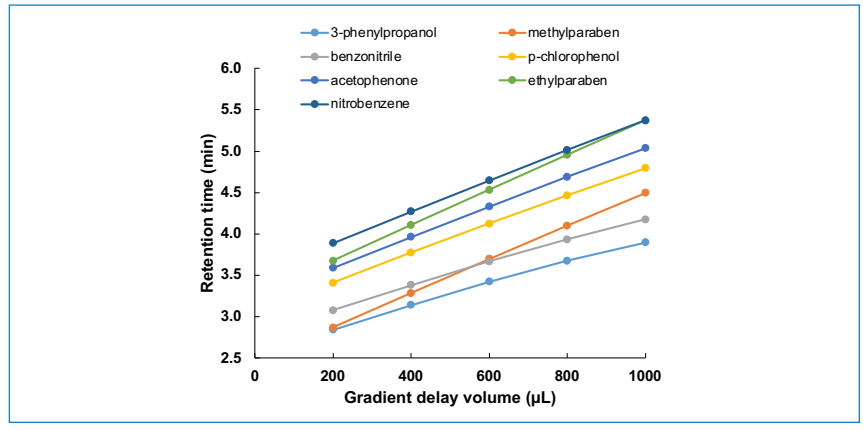

FIGURE 3: Dependence of retention time on gradient delay volume for several small molecules, obtained from simulations (www.multidlc.org/hplcsim). Chromatographic Parameters: Stationary phase, C18; Column dimensions, 50 mm x 2.1 mm i.d. (5 µm particle size); Flow rate, 0.4 mL/min; Temperature, 40 °C; Gradient elution from 10-50 %B from 0-5 min; A solvent, water; B solvent, acetonitrile. Red circles indicate coelution of 3-phenylpropanol and methylparaben (GDV = 200 µL) or methylparaben and benzonitrile (GDV = 600 µL); the green circle indicates that all three compounds are separated when the GDV = 360 µL.

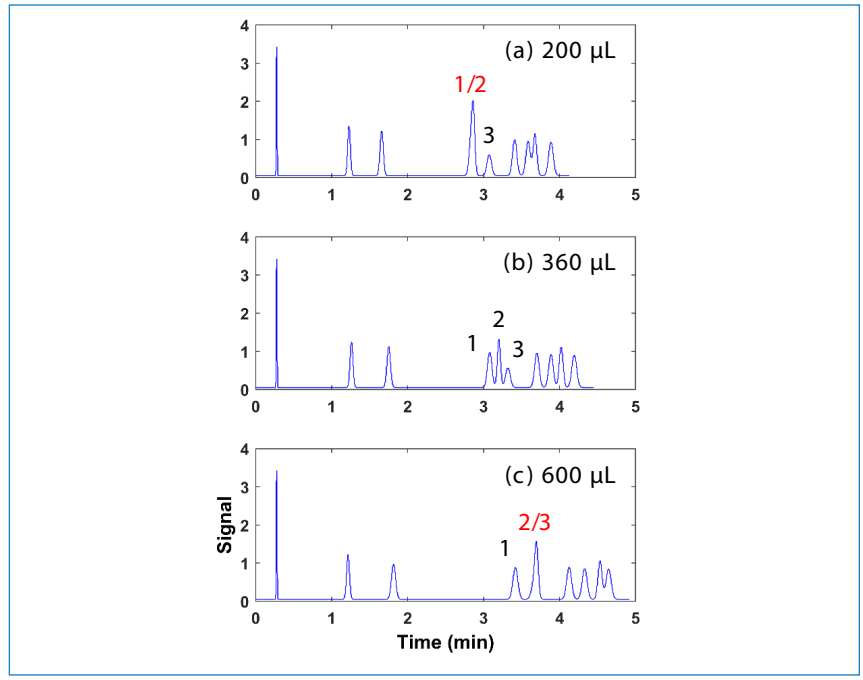

FIGURE 4: Simulated chromatograms highlighting the influence of GDV on separation selectivity and resolution. Conditions are the same as those described in Figure 3. In panels (a) and (c) we see that there is coelution of compounds 1 and 2 or 2 and 3, but in (b) we see all three molecules separated with a GDV of 360 µL. Compounds 1, 2, and 3 are 3-phenylpropanol, methylparaben, and benzonitrile.

Some Practical and Non-Ideal Aspects of this Framework

How Can I Measure the Gradient Delay Volume for My LC System?

It is most common to determine the GDV for a LC system experimentally by spiking one mobile phase solvent with a tracer compound that can be detected easily and used as a proxy for the actual mobile phase composition. A commonly recommended setup for this is to use water as Solvent A and 0.1% acetone spiked into water as Solvent B. Then, after removing the LC column from the system, a gradient is run from mostly A to mostly B, and the absorbance of the column eluent is recorded at a wavelength where the tracer absorbs. This produces a result like the dashed trace in Figure 2 (see Figure 4 of reference 2 for an example of a real experimental result). When we make GDV determinations in my laboratory, we typically use 50:50 acetonitrile:water for Solvents A and B, and spike Solvent B with 10 µg/mL of uracil. We prefer to have some organic solvent in A and B to reduce adsorption of the tracer to system components, and we prefer uracil over acetone because uracil is quite stable in

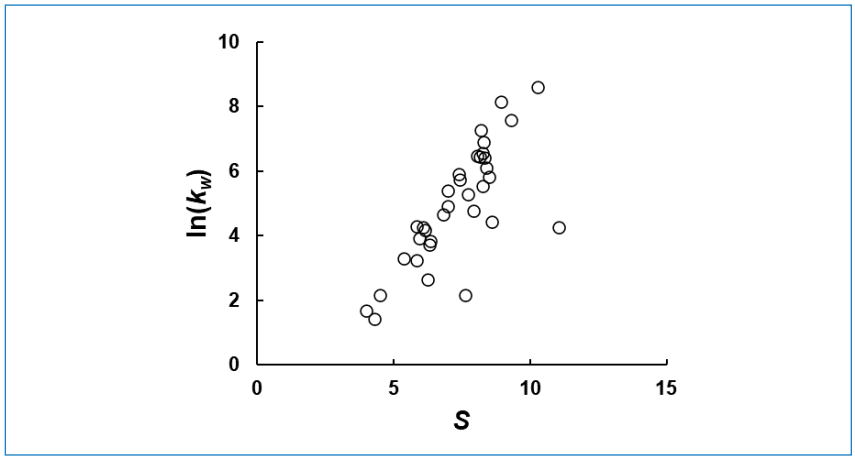

FIGURE 5: ln(k_w) and S values for the 40 small molecules preloaded in our HPLC simulator.

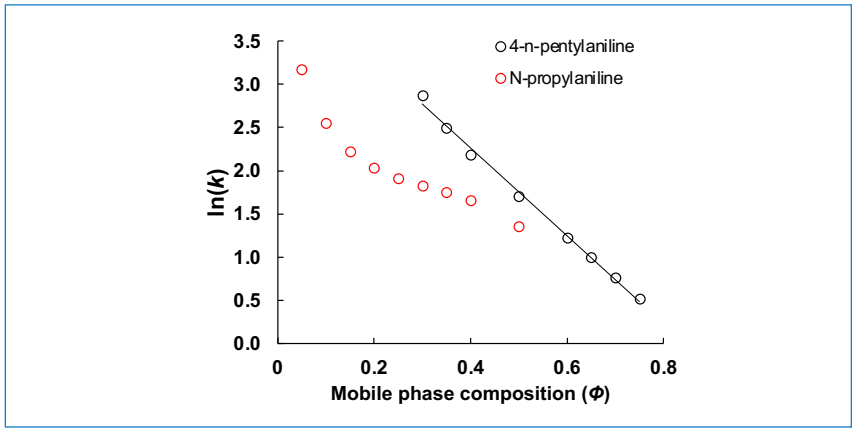

FIGURE 6: Experimental retention data for two small molecules illustrating varying degrees of linearity with respect to mobile phase composition. Conditions are the same as in Figure 3, except that mobile phase Solvent A is 25 mM ammonium formate, pH 3.2 (9).

solution (unlike the volatile acetone), and these solutions can be used reliably over many months.

How Do I Know What the *S* and ln(k_w) Values Are for the Compounds I'm Working With?

Figure 5 shows a plot of ln(k_w) and *S* values calculated from experimental retention data for the same small molecules that are loaded into our HPLC simulator (www.multidlc.org/hplcsim). We see that they are correlated, and they give us a sense for the range of values typical of small molecules. However, I am not aware of any models that can predict the values for any combination of molecule, stationary phase, mobile phase, and operating conditions with enough accuracy to simulate separations of closely related compounds; at this point in time, the values must be determined by experiment, from retention data collected under either isocratic or gradient elution conditions. Readers interested in this process are referred to recent work that both discusses the process and its limitations (6).

Is ln(*k*) vs. ϕ really always linear?

We observe very often that plots of ln(*k*) vs. ϕ are quite straight, at least over a range of ϕ relevant to practical separations, for small molecules and many biomolecules. An example of this is shown in Figure 6 for 4-n-pentylaniline. Sometimes, though, we observe that the relationship is nowhere near straight, as demonstrated in Figure 6 with the data for N-propylaniline, under exactly the same conditions. Building a highly accurate model in situations like this will require a non-linear model (for example, see the model of Neue and Kuss [7]); however, fitting even data like this to a linear model is good enough to support method development, provided that the user does not try to apply the model under conditions that are too far from the conditions used to collect the initial retention data (8).

Summary

In this installment of "LC Troubleshooting," I've discussed the concept of gradient delay volume (GDV) and our understanding of its impact on retention and selectivity in reversed-phase separations, primarily from a theoretical point of view. The dependence of retention and selectivity on GDV can be leveraged to good effect during method development, but this same dependence can cause trouble during method transfer. In next month's installment, I'll discuss the practical implications of these aspects in more detail, including tips for troubleshooting problems related to the GDV, and best practices for avoiding GDV-related problems by transfer-proofing new methods during development. ■

This article has additional supplemental information only available online.
Scan code for link.

ABOUT THE AUTHOR

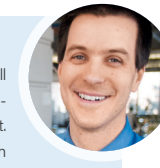

Dwight R. Stoll
is the editor of "LC Troubleshooting." Stoll is a professor and the co-chair of chemistry at Gustavus Adolphus College in St. Peter, Minnesota. His primary research focus is on the development of 2D-LC for both targeted and untargeted analyses. He has authored or coauthored more than 75 peer-reviewed publications and four book chapters in separation science and more than 100 conference presentations. He is also a member of *LCGC*'s editorial advisory board.

LCGCedit@mmhgroup.com

HALO®

A BETTER PATH TO SEPARATIONS

Meet HALO® PCS C18

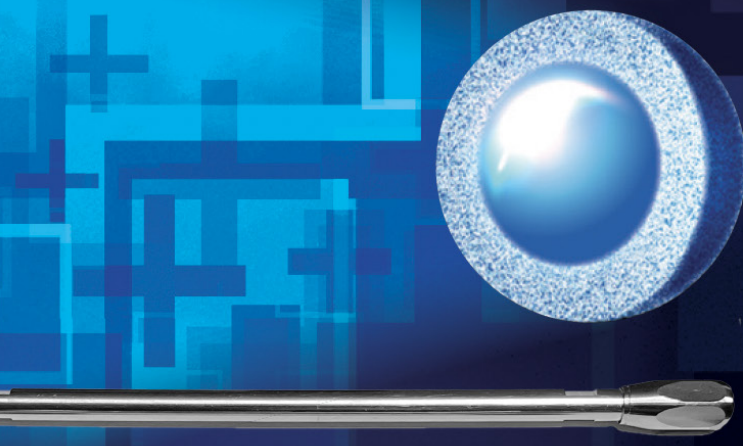

Peptide

C18

Basic

Compounds

Positively

Charged

Fused-Core®

- ✔ Excellent peak shape and increased loading capacity for basic compounds
- ✔ Ideal for use with low ionic strength mobile phases with UHPLC and LCMS compatibility
- ✔ Pore sizes available for both small molecule and peptide analysis

TRY HALO® PCS IN YOUR LAB

halocolumns.com | advancedmaterialstechnology

From Detector to Decision, Part III: Fundamentals of Calibration in Gas Chromatography

Nicholas H. Snow

Gas chromatography is a premier technique for quantitative analysis. As gas chromatographs have become simpler to use and data systems more powerful, much of the data processing involved in delivering quantitative results now happens in the background and is seemingly invisible to the user. In this installment, we will review the calibration techniques used with gas chromatography. We will compare calibration methods and the assumptions that underlie them. We will explore common mistakes and challenges in developing quantitative methods and conclude with recommendations for appropriate calibration methods for quantitative problems.

IN TWO PREVIOUS installments relating to detection and data analysis, we examined how detectors generate signals and how instruments can be operated remotely (1,2). We saw that, in today's gas chromatographs, there are many operations that happen in the background that can impact data analysis. In this installment, we examine another operation that often happens in the background: calibration and techniques for generating quantitative data.

For quantitative data analysis in gas chromatography, there are five commonly used techniques, summarized in Table I. Area percent normalization and area percent normalization with response factors are both simple and use, only the area percent report generated along with the chromatogram is needed. External and internal standard quantitation both involve the generation of a calibration curve. Finally, standard addition, as the name implies, involves addition of standardized quantities of the analyte of interest to samples. Each of these methods has advantages and limitations, which we will discuss below.

A typical integration report, which provides the retention time, peak height and area, peak width, area percent, and, if this information has been included in the method, an identification of each peak in a chromatogram, is shown in Table II. Classically, when the data system was a strip chart recorder, peak height was often used for quantitation, as this was much more easily measured by hand than peak area. With today's digital systems easily integrating the peaks, peak area is now almost exclusively used for quantitation, although the height is often still included in the default report on most data systems. In our next installment, we will discuss the principles of peak integration.

Area Percent Normalization

The most classical and simplest quantitation method is to simply equate the reported area precent of each peak to the mass or concentration percent in the sample. Although this is very simple, it involves several assumptions that can easily lead to inaccurate results. Most importantly, it assumes that the detected peaks are the only components present in the injected sample. There is no accounting for undetected analytes. It also assumes that all of the peaks are pure, and, finally, it assumes that the detector provides the same response for all analytes.

While area percent normalization is no longer widely used for direct quantitation of analytes, the basic principle is still used in many industries in which impurities or contaminants in finished products, such as pharmaceuticals, must be investigated if detected. Detection protocols for impurities are often based on a percentage of the peak area of the compound of interest. For example, such a protocol might require investigation of any unknown or impurity peak with a peak area greater than 1% of the compound of interest.

Area Percent Normalization with Response Factors

Area percent normalization can be used with detector response factors to mitigate errors due to variable detector response. Response factors, which correct the detector response based on comparison of the analyte of interest to a standard analyte, such as hexane, are used to correct for detector response variability. Table III shows an area percent normalization with response factor calculation for the same mixture seen in Table II. Corrected peak areas are generated by multiplying the raw peak areas by the response factor. Corrected area percent values for each peak are then calculated from the corrected peak areas. As seen in Table III, response factors for flame ionization detection (FID), which most analysts think of as counting carbon atoms, indicate a much more complex mechanism for generating signals. The corrected area percent values seen in Table III differ considerably from the raw area percent values shown in Table II.

In this case, the raw peak areas are corrected using the response factors to generate a far different quantitative view of the sample than seen by just using the original peak areas. While this method presents a more accurate analysis, it still suffers from the assumption that the peak areas determined by the data system represent all components in the sample. It is also still subject to variability in analyte recovery in the sample preparation and injection processes.

TABLE I: Summary of calibration methods for gas chromatography

Technique	Assumptions
Area Percent Normalization	All components in sample show peaks Detector has same response for all components All components undergo same extraction recovery All components undergo same injection behavior
Area Percent Normalization with Response Factors	All components in sample show peaks All components undergo same extraction recovery All components undergo same injection behavior
External Standard Calibration	All components undergo same extraction recovery All components undergo same injection behavior
Internal Standard Calibration	Internal standard and analytes undergo same precision in extraction recovery and injection behavior Internal standard cannot be a sample component
Standard Addition	Response is linear at all masses and concentrations

TABLE II: A typical area percent integration report

Peak Number	Retention Time (min)	Height	Area	Width (min)	Area Percent (%)
1	2.375	1753	15234	0.10	15.39
2	3.456	2123	20927	0.10	21.15
3	4.576	975	9321	0.11	9.42
4	5.123	3045	28723	0.11	29.02
5	6.041	2523	24757	0.12	25.02
TOTAL		**10,419**	**98,962**		**100.00**

TABLE III: Area percent normalization with response factor calculation

Peak Number	Raw Peak Area	Response Factor	Corrected Area	Corrected Area Percent (%)
1	15,234	0.64	9,750	11.7
2	20,927	0.90	18,834	22.5
3	9,321	0.78	7,270	8.7
4	28,723	0.79	22,691	27.2
5	24,757	1.01	25,005	29.9
TOTAL	**98.962**		**83.550**	**100.0**

External Standard Calibration

External standard is the classical calibration method that we all learned as undergraduates. To generate a calibration curve, the signal, in our case peak area, is plotted as the dependent (y) variable against the concentration or mass of analyte injected as the independent (x) variable on a two-dimensional plot. Nearly all chromatographic detectors provide a linear response versus concentration or mass over a specified range. While detector linear range and response are not discussed in detail here, the are discussed in previous installments, on ChromAcademy, *LCGC International*'s online training platform and in numerous textbooks (3–5). A typical external standard and calibration curve is shown in Figure 1.

In contrast with the two area percent normalization techniques, an external standard calibration requires that several standards, in addition to the analyte samples, be run to determine the calibration curve. In Figure 1, each data point represents a standard that was analyzed in addition to any analyte samples. Due to differences in response factors, if there is more than one analyte of interest in the sample, separate calibration curves would be needed for each analyte.

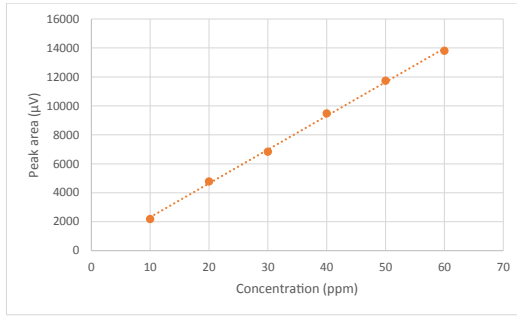

FIGURE 1: External standard calibration curve. Peak area is plotted against mass or concentration of injected analyte standard.

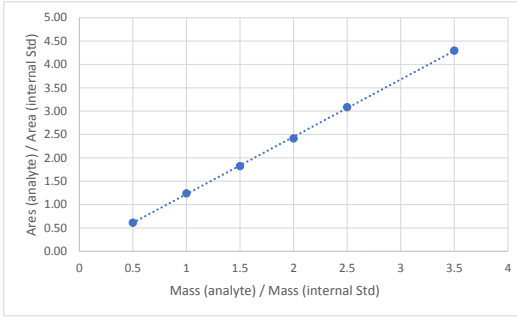

FIGURE 2: Internal standard calibration curve. Peak area ratio of analyte to internal standard is plotted against mass or concentration of injected standard.

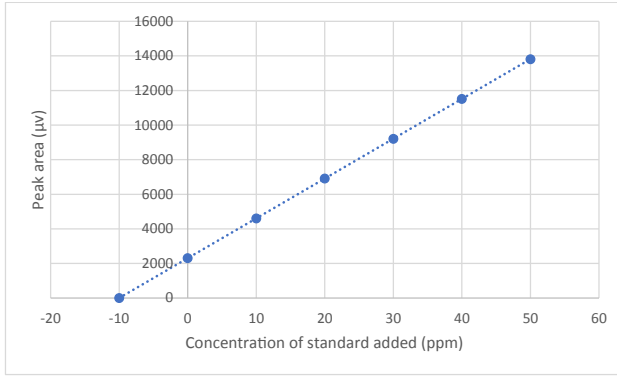

FIGURE 3: Standard addition calibration. Peak area of samples with added aliquot of standard is plotted against added aliquot of standard.

While external standard calibration mitigates the need to consider response factors and does not assume that the components of interest are the only components in the mixture, it does suffer from experimental uncertainty that may arise from sample preparation and injection. Most sample preparation and extraction techniques that are more complicated than "dilute and shoot" may introduce unacceptable variation, often on the order of 10% or more, relative, on the amount of analyte extracted. This translates into a similar uncertainty in the calibration curve. Furthermore, classical injection techniques, such as split or splitless, may also introduce several percent additional relative experimental uncertainty. In short, external standard calibration curves in gas chromatography are often very noisy, and may not meet statistical linearity requirements for regulated laboratories. Today's inlets and autosamplers generally provide much better reproducibility than in the past, somewhat mitigating this problem.

Internal Standard Calibrations

When external standard calibration is subject to experimental errors due to variability in analyte extraction during sample preparation and injection, internal standard calibration can mitigate these problems. Before discussing internal standard calibration, we should note that the uncertainties and errors that exist in the external standard method still exist in the internal standard method, except that the internal standard method corrects for them by dividing the variability out in the calculation.

An internal standard is a known mass or concentration aliquot of a compound that does not, and cannot, appear in any of the samples (that is, added to all samples and standards) prior to sample preparation or extraction. Since it is added to all samples and standards, the internal standard is then subjected to the same extraction and injection process as the samples and standards. When a calibration curve is generated, the peak areas for the compound of interest are ratioed with the peak area of the internal standard, prior to plotting on the curve. A typical internal standard calibration curve is shown in Figure 2. The peak area ratio of analyte to internal standard is plotted against the known mass or concentration of the analyte in the standards. For analyte samples, the peak area ratio is calculated and the mass or concentration of the analyte is read from the calibration curve or calculated using the equation for the line.

Internal standard calibration mitigates variations in analyte extraction recovery and injected quantity from sample-to-sample by dividing the peak

TOSOH

TRIPLE DETECTION FOR ADVANCED POLYMER CHARACTERIZATION

GPC/SEC systems for all applications

The EcoSEC Elite™ and EcoSEC™ High Temperature GPC systems deliver high stability and reproducibility for accurate polymer characterization.

Advanced GPC/SEC detectors with unique technology

The LenS™$_3$ MALS and the *NEW* LenS$_3$ MALS-V light scattering / viscometry dual detector offer a tailored solution for SEC-MALS and triple detection.

A team of experts supports your work

Our team of chromatography experts provides polymer scientists with solutions to develop and characterize safe materials for the future.

Contact us for more information:

800-366-4875 info.tbl@tosoh.com www.tosohbioscience.com

TOSOH BIOSCIENCE

areas obtained for the analyte be the peak area for the internal standard. It is assumed that the internal standard and analyte will behave the same through the extraction and injection processes. If there is low recovery of analyte, there should be the same low recovery of the internal standard. Likewise, the internal standard must behave similarly in the chromatographic column as the analyte, but not co-elute.

These ideas lead to several requirements for the internal standard that often make internal standard selection challenging.

- The internal standard cannot be a possible analyte, contaminant, or interference in the samples. If this happens, the peak area for the internal standard will be artificially large, leading to an artificially low calculated analyte concentration.
- The internal standard must undergo similar behavior and recovery in the extraction process. Internal standards with similar structural features as the analytes of interest are often chosen.
- The internal standard must undergo similar behavior and recovery through the injection process. It should be chosen to have similar inlet discrimination to the analytes.
- The internal standard peak must not overlap with any peaks in the standards or samples. The chromatography of the internal standard must be checked to ensure no peak overlap.
- The internal standard must be available at high and reproducible purity. If it is impure or of low quality, it may generate interfering peaks or have inconsistent peak area.

In gas chromatography-mass spectrometry (GC–MS), these problems are often solved by using a deuterated analog of the parent compound of interest. For example, in cannabis analysis, the main active component, Δ9-tetrahydrocannabinol can be analyzed alongside a d-3 analogue, which has the same shape and structure as the parent compound, except a 3 Da higher atomic mass, due to the replacement of three hydrogen atoms with deuterium. Deuterated analogs extract and traverse the column nearly identically with the parent compounds, with a slight difference in retention time. The peak overlap is solved in GC–MS using extracted ion chromatograms or selected ion monitoring to generate separate peaks for the parent compound and analogue. In non-GC–MS analyses, candidate internal standards must be analyzed until one that meets all the requirements is found.

Since the calculations are very similar and the data for external standard calibration is also collected when performing internal standard calibration, I often perform both during method development or troubleshooting. Ideally, the internal and external standard methods should give the same quantitative result and the same uncertainty. Differences in the quantitative results or uncertainty indicate potential hidden problems with the extraction or injection processes.

Standard Additions

Standard addition calibration can be used when the sample matrix is too complex to allow ready addition of an internal standard or when the baseline or other peaks may be interfering with the peak of interest. It can be used with either peak height or peak area and is one of the few instances in gas chromatography where peak height is often superior to peak area. A typical standard addition calibration curve is shown in Figure 3. First, the samples are run, and the peak(s) of interest are identified. A known mass or concentration aliquot of each analyte of interest is added to each sample and the sample is re-run. This procedure is repeated with successive additional known aliquots added to each sample.

Once enough aliquots to generate a line have been added, a separate plot of peak area versus amount of standard added is generated for each sample. The mass or concentration of analyte in the sample is then determined by extrapolating the line to the *x*-axis. In Figure 3, this extrapolation is seen in the data point to the left of the *y*-axis, showing negative values for the concentration. The actual concentration of the sample would be read as about 10 ppm.

Conclusions and Summary

Referring to Table I, the main calibration techniques for quantitative analysis by gas chromatography are, in order from simplest to most complex, area percent normalization, area percent normalization with response factors, external standard calibration, and internal standard calibration. Standard addition is used in situations where samples are too complex for the other techniques. Each method has built-in assumptions, advantages, and disadvantages. While the simple area percent methods are useful for estimations, due to their assumptions, they are not generally effective for accurate quantitative analysis. Internal standard calibration is usually more precise than external standard calibration, but can hide uncertainty and variability in the sample preparation and injection processes. An understanding of the fundamentals of calibration is critical in the detection to decision process.

ABOUT THE AUTHOR

Nicholas H. Snow

is the Founding Endowed Professor in the Department of Chemistry and Biochemistry at Seton Hall University, and an Adjunct Professor of Medical Science. During his 30 years as a chromatographer, he has published more than 70 refereed articles and book chapters and has given more than 200 presentations and short courses. He is interested in the fundamentals and applications of separation science, especially gas chromatography, sampling, and sample preparation for chemical analysis. His research group is very active, with ongoing projects using GC, GC–MS, two-dimensional GC, and extraction methods including headspace, liquid–liquid extraction, and solid-phase microextraction.

LCGCedit@mmhgroup.com

Connect with us on social media!

Stay up to date with unbiased, nuts-and-bolts technical information and news with a practical focus. Like and follow us on all our social media pages to never be left out of the loop.

LCGC™ INTERNATIONAL

chromatographyonline.com

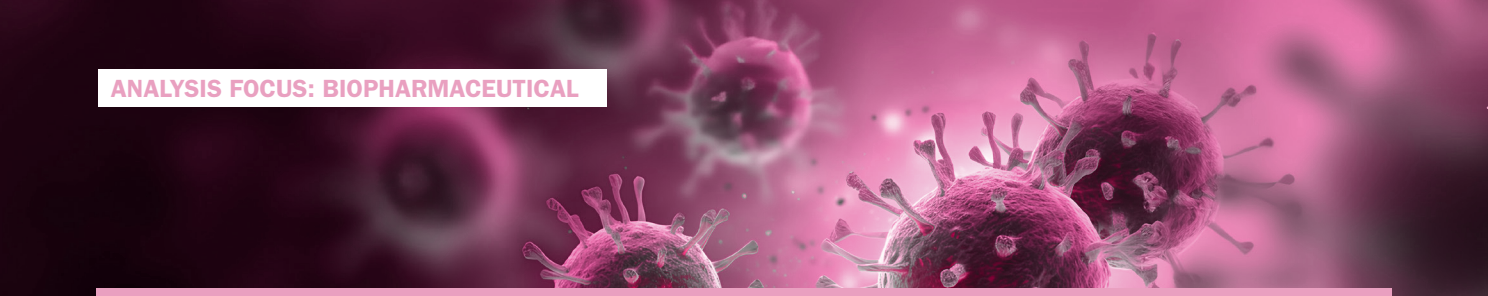

Trends in Biopharmaceutical Analysis: A Focus on Integrating Single-Cell Omics with Microfluidic Chips

Anantdeep Kaur, Jahziel Chase, Jared R. Auclair, and Anurag S. Rathore

Biopharmaceutical analysis is a rapidly evolving field that requires the development of new technologies and methods to keep pace with the increasing complexity of biologics. One of the most promising areas of research is the use of single-cell omics and microfluidic chips for the analysis of biopharmaceuticals. Single-cell omics has revolutionized our understanding of cellular heterogeneity, while microfluidic chips have enabled high-throughput analysis of single cells that provide an understanding of the complex biological network that complements the genomics and transcriptomics studies. This article will explore some of the emerging trends and technologies in biopharmaceutical analysis, with a particular focus on single-cell omics and microfluidic chips. We will also discuss the developments in ambient ionization mass spectrometry such as sub nanoampere ionization and the potential of low current ionization in studying cell-to-cell heterogeneity and its role in metabolomics.

VARIATIONS DISPLAYED by the cell populations in their DNA, RNA, proteins, and metabolites lead to significant heterogeneity and differences in cell states (1). An understanding of the cell-to-cell variations can help reveal the physiological and pathological processes such as disease progression (2). While traditional methods in cell analysis have overlooked cell-to-cell variations that contribute to drug resistance, the development of single-cell analysis methods has enabled remarkable progress in clinical and biomedical research particularly in drug development (3).

While the molecular copy numbers of nucleotides, proteins, and metabolites in single cells are low, the dynamic range is wide; therefore, highly sensitive single cell sample preparation methods are of great value for single cell analysis (4). In this regard, microfluidics has emerged as an important tool in single-cell analysis with the advantages of cost effectiveness, automation, miniaturization, and high throughput ability (5,6).

In recent years, there has been a growing interest in integrating single-cell omics with microfluidic chips for the analysis of biopharmaceuticals (7,8). This approach has several advantages over traditional methods of biopharmaceutical analysis, as it allows for a high degree of automation and allows for high-throughput studies due to its ability to perform multiple assays on a single chip. Minimum amounts of reagents are required, reducing assay cost, and improved sensitivity is achieved by using microchannels that provide a higher surface-area-to-volume ratio. The multiple unit microfluidic chip allows for the different processes of cell injection, culture, capture, lysis, and detection to be completed in a single microfluidic chip. In addition, multiple structures can also be included in a microfluidic chip to capture single cells. At a drug discovery level, microfluidics can help in identification, characterization, purification, and structure elucidation of chemical moieties (9). Drug screening can achieve high throughput, cost-effective, and rapid increase in the rate of sample analysis using microfluidics.

A microfluidic chip is mostly fabricated with elastomers, inorganic materials, and thermoplastics for either droplet microfluidics, microwell arrays, or hydrodynamic microfluidics (such as S-shaped microchannels). The commonly used fabrication materials include polydimethylsiloxane (PDMS), silicon, glass, quartz, polycarbonate, and polymethylacrylate (PMMA). The chip comprises of a reagent inlet, sample inlet, valves, microchannels, the drainage system, and the sensor part (10). Based on the flow of fluids, microfluidic chips can be classified into three main types: traps-based microfluidics (11), valves-based microfluidics (12), and droplet-based microfluidics (13).

Microfluidic Chips for Single-Cell Analysis

Microfluidic chip design helps in efficient sample isolation, cell sorting, lysis, and protein digestion, while liquid chromatography tandem mass spectrometry (LC–MS/MS) is the leading tool for protein identification and quantification (14). Single cell isolation can be achieved using droplet microfluidic chips wherein single cells are encapsulated within individual droplets, mainly by using an intersection of immiscible phases such as water-oil droplets in microchannels or through capillary tips (15). Further sorting and analysis of the cells is achieved by labeling of the single cells in droplets coupled with analytical methods such as biochemical reactions and fluorescence microscopy that enable real-time single cell detection. Recently, rapid droplet formation was achieved by constructing a micro cage array platform that contains multiple micropillars that can rapidly spread the oil phase through gaps between the pillars to trap droplets (16). Another method of achieving single cell isolation is by using microwells that can only accommodate one cell. The cell suspension is loaded onto the microwell array and single cells settle into each microwell due to gravity. Microwell arrays are a useful platform for studying the effects of drugs on single cells (17). Pang and associates investigated drug resistance of single-cell-derived tumor sphere based on an integrated microfluidic device. Single glioblastoma cells were isolated, captured, and then cultured into single cell derived spheres. Vincristine, the anti-cancer drug, was infused and co-cultured with the tumorspheres. The study showed that tumorspheres derived from smaller and more easily deformed tumor cells showed higher drug resistance (18).

While microwells employ physical boundaries to capture single cells, hydrodynamic trapping in microfluidic systems captures single cells by using specific fluid flows using cup-shaped micropillars (19) and S-shaped microchannels (20). Cup-shaped micropillar is one of the most used microstructures to isolate and trap single cells. Single cell trapping is achieved by covering the gap in a micropillar that reduces the fraction of fluid streamlines that can flow into the trap. Microfluidic chips with cup-shaped micropillars have been shown to achieve an isolation efficiency greater than 95% for isolating single floating cancer cells (21).

Microfluidic Chip Coupled for Single-Cell Omics Analysis

Single-cell multi-omics, including transcriptomics, proteomics, metabolomics, and lipidomics, help to comprehensively understand cellular characteristics and cellular regulatory networks. The key requisite for the downstream analysis of sin-

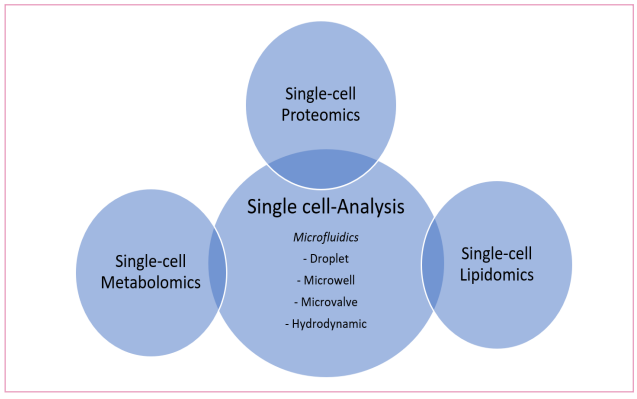

FIGURE 1: Microfluidics coupled with MS for single cell proteomics, metabolomics and lipidomics analysis. Figure adapted from reference (2).

gle cells is the ability to be able to precisely manipulate single cells in microfluidic channels. Single-cell omics poses challenges to sampling techniques and MS sensitivity. Compared with single-cell metabolomics and lipidomics, single-cell proteomics has been more explored. Droplet microarray is one of the most suitable platforms for single-cell proteomics preprocessing, and has been used to understand cell phenotype differences and inter-relationships between functional networks (22).

The droplets encapsulate the sample that provides compartments for extraction and digestion of proteins. This prevents overdilution of samples, and reduces the time for digestion (23). Comprehensive characterization of single cell proteome using sensitive MS is possible using single-cell sorting sample preparation from microfluidics, and provides detailed information of protein post-translational modifications as well as signal transduction-related functional proteins, such as transcription factors, kinases, receptors, and surface antigens.

Microfluidic chips, composed of droplet microfluidics, arrays of microwells, arrays of micropillars, microchannels in special structures, and microvalves, can be used alone or in combination with bioanalytical assays to efficiently isolate and capture single target cells. Such a microfluidic platform has been used to sort immune cells, followed by lysis and digestion in centrifuge tubes for proteomic analysis. By using nano-LC–MS, 346 to 911 and 275 to 549 proteins were identified from 1000 and 100 THP-1 cells, respectively (24).

Gebreyesus and associates developed a streamlined and robust workflow that combined microfluidics and proteomic analysis based on data independent acquisition (DIA) MS for single-cell proteomic analysis, cell trapping, cell lysis, protein digestion, and peptide desalting to be performed on a single chip. The peptides collected from the chip were further analyzed using LC–MS/MS in DIA mode. 100 ± 131 protein groups were identified by the chip-DIA workflow from a single cell (25).

Due to the dynamic nature of metabolites to the environment, variations in metabolic status during analysis is a key area of concern. There are mainly two strategies for single cell metabolomic analysis; either analyzing intact cells directly by MS, or extracting metabolites from cells prior to MS detection (26,27). In recent work, a serpentine channel microfluidic chip was integrated with a pulsed electric field-induced electrospray ionization-high resolution MS (PEP-ESI-HRMS) to analyze single-cell metabolite (28). The asymmetric serpentine channel helped in continuously isolating single cells. Pulsed square wave electric filed was then applied to disrupt single cells and trigger ESI. Using the PEP-ESI-HRMS system, 80 cells could be analyzed in a minute, with about 120 metabolites identified per single cell. Microfluidic chips designed with narrow and long microchannels that allow only single cells to pass through can be used for cell delivery (29). Under a direct current voltage, single cells isolated in the microchannel can be lysed and ionized for MS analysis. The single-cell analysis platform can analyze about 40 cells per minute, and identify ≈100 metabolites from a single cell. The methodology led to the identification of 67 endogenous metabolites from single K562 cells (30). Similar with single cell metabolomic analysis, single-cell lipidome can also be analyzed using capillary ESI-MS to detect hundreds of lipid molecules with high resolution and accuracy. Single-cell metabolomics differs from lipidomics in the polarity of molecules; therefore a different solvent system is used for single-cell lipidomics. One of the challenges in single cell lipodomics is the complexity arising

due to a large number of isomers of lipids. One possible solution is to integrate PB reaction with tandem MS to achieve the quantification of double bond position isomers in lipids (31,32).

The microfluidic MS-based single-cell omics has shown to have great potential in biomedical and clinical studies. It can help in revealing the heterogeneity of cells that is critical to study the progression of cancers, investigating the effect of drugs on the immune system as well as aid in understanding drug resistance during therapy (33,34). In addition, the characterization of single cell omics has the potential in the discovery of disease biomarkers.

Low Current Ionization in Studying Cell-to-Cell Heterogeneity

Ambient ionization refers to the ionization of unprocessed or minimally modified samples in their native environment, and it typically refers to the ionization of condensed phase samples in air. Ambient ionization MS techniques can be largely categorized into three classes based on their desorption method: liquid extraction, plasma desorption, and laser ablation. Ambient ionization MS techniques have been used for high-throughput analysis of clinical samples, including human biofluids, particularly for rapid therapeutic drug monitoring as well as to quantify drugs in cell cultures and tissue sections. This is mainly attributed to the ability to conduct the direct analysis of samples in their native environment without needing sample preparation (35).

Recent developments in ambient ionization mass spectrometry, such as sub-nanoampere ionization, have shown promise in studying cell-to-cell heterogeneity and its role in metabolomics. *Sub-nanoampere ionization* is a type of ambient ionization mass spectrometry that uses low currents to ionize samples. This approach has several advantages over traditional ionization methods, including the ability to analyze small numbers of cells along with the ability to analyze samples in their native environment. As an example, the pressure probe electrospray ionization MS with internal electrode capillary (IEC-PPESI-MS) can be integrated for high spatial resolution sampling and precise post sampling manipulation for single-cell analysis (36,37).

Another promising technology is paper spray ionization, which is a type of ambient ionization mass spectrometry that uses paper as a substrate for sample analysis. A paper triangle wetted with non-polar solvents such as hexane produces a spray of non-polar solvent droplets when a relatively low positive or negative voltage (0.8 ≈ 2 kV) is applied. The spray occurs at the tip of the paper, and is presumably due to field-assisted evaporation, while the solvent is transported as a result of capillary action through the micro-channels in the paper substrate (38).

This gentle method of ionization is applicable to a wide range of biological compounds including peptides, small nucleotides, phospholipids, and other compounds. This approach has several advantages over traditional ionization methods, including the ability to analyze small numbers of cells and the ability to analyze samples in their native environment by (i) low detection limits; (ii) low internal energy deposition; and (iii) compatibility with prior experiments that require aqueous or polar solvents, including prior chromatographic separations (39).

In a recent study, researchers used femto-flow electrospray ionization (ESI) with flow rates ranging from 240 fL min^{-1} to the low pico level (<10 pL min^{-1}) using a submicron emitter tip and relay ESI configuration to analyze single cells. The researchers obtained high-quality mass spectra from single cells, which allowed them to identify metabolites not detectable using traditional methods (40).

Compared with nanoESI, femto flow ESI exhibits lower ion current intensities (>2 orders of magnitude lower), ionization currents <218 pA, and lower flow rates (>3 orders of magnitude lower). The femto flow ionization technique allows the use of highly concentrated sample solutions in regular MS analysis, thereby removing the need for dilution when lower intensity ion beams are needed. Thus, for a non-buffered protein solution, the low flow ionization modes allow native charge states to be produced in an either charge-enhancing or charge-reducing manner. The measured flow rates and ionization currents then allow for the calculation of the size of initial charged nanodroplets. These techniques have the potential to revolutionize biopharmaceutical analysis by enabling the analysis of small numbers of cells in a cost-effective and efficient manner (41). ■

This article has additional supplemental information only available online.
Scan code for link.

ABOUT THE AUTHORS

Anantdeep Kaur
is a Postdoctoral Research Associate at the Biopharmaceutical Analysis Training Laboratory for the Department of Chemistry and Chemical Biology at Northeastern University, in Boston, Massachusetts.

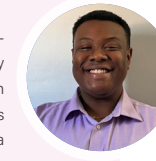

Jahziel Chase
is a third-year PhD candidate, candidate in the Department of Chemistry and Chemical Biology at Northeastern University, specializing in protein mass spectrometry. After graduating with a B.S. in Biochemistry from the University of Massachusetts Amherst in 2021, Jahziel Chase has dedicated his academic career to the field of mass spectrometry.

ABOUT THE EDITORS

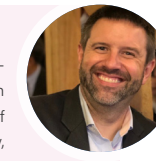

Jared R. Auclair
is Interim Dean at the College of Professional Studies, Vice Provost Research Economic Development and Director of Bioinovation at Northeastern University, in Boston, Massachusetts. He is also the Director of Biotechnology and Informatics, as well as the Director of the Biopharmaceutical Analysis Training Laboratory.

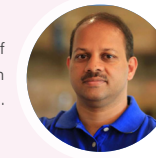

Anurag S. Rathore
is a professor in the Department of Chemical Engineering at the Indian Institute of Technology in Delhi, India.

PEER REVIEWED

LCGC International papers have undergone a peer review process and are available on our open-access website.

Liquid Chromatographic Peak Purity Assessments in Forced Degradation Studies: An Industry Perspective

Pascal Marillier, Neal Adams, Steven W. Baertschi, John M. Campbell, Chris Foti, Juçara Ribeiro Franca, Simon Hicks, Dorina Kotoni, Christian Laue, Stacey Marden, Liping Meng, Ana Claudia de Oliveira Santos, Mariah Ultramari, An Van Cleempoe, Chloe Wang, Todd Zelesky, and Zongyun Huang

This review article discusses scientific rationales and current best practices in the pharmaceutical industry for performing chromatographic peak purity assessments (PPA). These activities are associated with the development and validation of liquid chromatographic (LC) stability-indicating analytical methods applicable to regulatory submissions of small-molecule drug candidates. The discussion includes a comprehensive overview of the PPA-related regulatory and scientific landscape and common industry approaches to obtain PPA results, as well as the strengths and weaknesses of PDA-facilitated ultraviolet (UV) PPA and other PPA techniques.

THE EXECUTION of chromatographic peak purity assessments (PPAs) is associated with the development of stability-indicating analytical methods (SIM) applicable to regulatory submissions (marketing applications) by pharmaceutical companies. When developing these methods, a forced degradation study (FDS) assessment is required to demonstrate that the method can adequately assess the stability of drug substances (DS) and drug products (DP) (1-4). The quality of the FDS data is dependent upon a well-designed FDS with scientifically justified conditions as well as appropriate evaluation of pertinent qualitative and quantitative FDS data, including correlations with mass balance data. If the quality of the data acquired during the FDS is sufficiently high, then the study informs our understanding of the stability-indicating capabilities of the analytical method.

When FDS data are compiled and analytical measures such as system suitability test and mass balance results indicate acceptable quality, the method is still at risk of having inadequate stability-indicating capability if pharmaceutically relevant degradant peaks coelute with the parent peak in stressed sample chromatograms. Such risks can be mitigated by evaluating the purity of the peak representing the main (parent) analyte; such an evaluation can be performed using various techniques where photodiode array (PDA)-facilitated PPA is most commonly employed (5). Although health authorities (HAs) in some countries require that the "chromatographic purity of the analyte signal" (that is, spectral homogeneity) shall be demonstrated for chromatographic methods (6,7), the requirement, as written, does not present specific expectations and guidance on the appropriate means to demonstrate peak purity.

Nevertheless, a PDA-facilitated PPA has become the de facto interpretation of how to assess peak purity by HA reviewers, evidenced by consistent requests for software-calculated peak purity data in queries received from various HAs regarding regulatory submissions containing chromatographic methods with ultraviolet (UV) detection. Notably, the draft ICH Q2(R2) guideline only states "spectra of different components could be compared to assess the possibility of interference" as an alternative to "suitable discrimination" in the Specificity/Selectivity section (4.1) without any specific mention of PDA-facilitated PPA. Although peak purity tests are not mentioned in the revised ICH Q2(R2) draft (8,9), ICH Q2(R1) states that "peak purity tests may be useful to show that the analyte chromatographic peak is not attributable to more than one component (diode array, mass spectrometry)." This statement, however, does not mandate PDA-facilitated PPA or any other specific technique for demonstrating method selectivity,

GL Sciences
https://www.glsciences.com/

Optimize your PFAS testing


SPE Cartridge


Gas Purifier


Delay Column

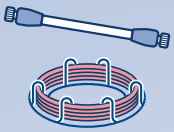
LC/GC Column

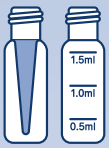

Vial


Air Sampler

PFAS Testing Solution

SPE Columns

- InertSep WAX Mix Mode Anion Exchange
- InertSep MA-2 Anion Exchange
- InertSep PLS-2 SDVB
- InertSep GC Graphite carbon

Delay Column

- Delay Column for PFAS,
  Packed with High Purity Graphite Carbon Beads

LC Column

- InertSustain AQ-C18

Accessories

- PTFE free Gas Purifier
- High Purity Polypropylene Vial / Cap with aluminum septa

TABLE I: Example chromatography data systems and peak purity criteria

Vendor	Software Brand	Criteria for Pure Peak
Waters Corp.	Empower	Purity angle (θ) < Purity threshold
Agilent	OpenLab CDS	Purity value (1000 x $\cos^2\theta$) > Purity threshold
Shimadzu	LabSolutions	Purity index ($\cos\theta$) > Purity threshold
ThermoFisher/Dionex	Chromeleon	Purity index ($\cos\theta$) > Purity threshold
Gilson	Trilution	Purity value (1000 x $\cos^2\theta$) > Purity threshold
Knauer	ChromGate	Similarity index > Purity threshold

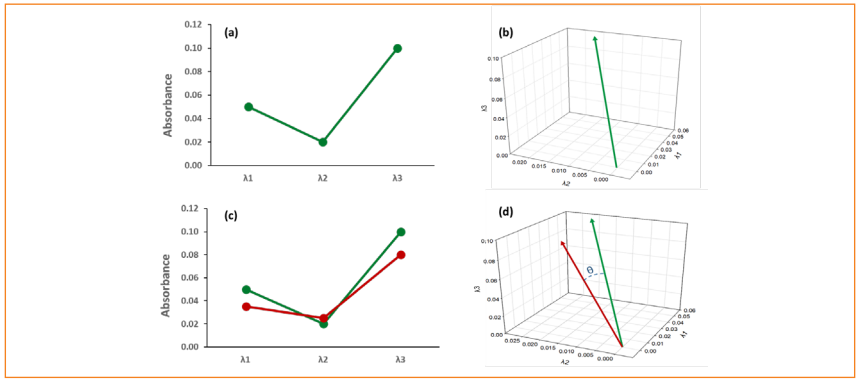

FIGURE 1: Graphical representation of absorbance vs. wavelength in dimensional space (reproduced from Figure 1 in [10]): (a) Depiction of a three-point spectrum; (b) representation of this spectrum as a vector in 3D space; (c) depiction of two, similar three-point spectra; (d) representation of these two spectra as vectors in 3D space, with the angle between the vectors representing spectral similarity.

and it is not regarded as a universal requirement by HAs and companies (although it is often a good practice).

PDA-facilitated (or, interchangeably, UV spectral) PPA is just one technique for demonstrating selectivity in a stability-indicating method. Several other valid techniques, including performing mass spectral PPA, spiking impurity markers, employing orthogonal chromatographic conditions, or using two-dimensional liquid chromatography (2D-LC), can effectively evaluate peak purity without relying solely on PDA-facilitated PPA. With a focus on small molecule active pharmaceutical ingredients (APIs), it is important to note that there is no universally appropriate technique for assessing selectivity. The most suitable technique should be selected on a case-by-case basis, supported by scientifically sound reasoning. Factors such as the chromatographic separation technique, detector type, and specific characteristics of the molecules of interest must be considered. Note that, because of the limitations mentioned above, PPA never proves unequivocally that a peak is pure. Rather, PPA can only be used to conclude that no coeluted compounds were detected. Combining a PPA along with other characteristics of forced degradation (including relevance of the specific degradation pathway) and validation greatly increases the confidence in the stability-indicating nature of the analytical method.

The absence of specific regulatory guidance on PPA poses challenges for both HA reviewers and applicants in terms of understanding the process of demonstrating method selectivity, setting appropriate acceptance criteria, and including sufficiently documented evidence of having met those criteria. To advocate for a shared understanding between industry and HA, the goal of this paper is to provide science-based clarification to guide LC-based PPA activities in the pharmaceutical industry, especially as it relates to small molecule APIs.

This article primarily centers around PDA-facilitated UV PPAs as the main tool for assessment, but it also explores additional supplementary techniques such as mass spectrometry (MS) and 2D-LC. Molecules with no chromophore (memantine) or where impurities commonly have essentially the same UV spectral characteristics (oligonucleotides), however, cannot be effectively evaluated using UV spectral PPAs, and hence, are not the focus of this article.

Peak Purity Assessment Options

The following are some examples of PPA assessment approaches.

PDA-Facilitated PPA

PDA-facilitated PPA is the most common approach to demonstrating adequate selectivity and is usually calculated using commercial chromatographic data systems (CDSs) or software, which examine changes in the UV absorbance spectrum throughout the peak to detect coeluted compounds with different UV absorbance spectra. A list of some commercially available PPA CDSs is presented in Table I. Commercial CDSs differ slightly in their spectral peak purity algorithms and terminology (10), but the core concepts to perform PPA are consistent—determining spectral contrast by comparing UV absorbance spectra at different points across the peak of interest to that of the apex. To describe the basic principles, the PPA method and terminology from Waters' Empower software (11) will be used as an example of a widely accepted CDS among pharmaceutical companies. As depicted in Figure 1, Empower measures spectral contrast (that is, the shape difference between two spectra) as follows:

1. Spectra are baseline corrected by subtracting interpolated baseline spectra between peak baseline liftoff and baseline touchdown.
2. Spectra are converted into a vector in *n*-dimensional space.
3. Vector lengths (concentration)

are minimized using least-squares regression.
4. The vectors are moved into a 2D plane and the angle between them is measured.

A spectral angle of 0 or 90 degrees indicates that the spectral shape is identical or that there is no spectral overlap, respectively. Spectra that diverge within a single peak are typically attributed to the coelution of compounds. Spectral contrast is used to compare all spectra within a peak to the apex spectrum by using an algorithm to calculate the purity angle (a weighted average of all calculated angles) and the degree of uncertainty because of the variation in the spectral vector (that is, the threshold angle) based on both solvent and noise contributions. A chromatographic peak is considered spectrally pure when its purity angle value is less than its purity threshold. Maziarz provides a practical example of verifying the spectral homogeneity of an API (12).

As listed in Table I, Agilent's OpenLab CDS software uses a comparable approach to assess peak purity by calculating a similarity factor, which is expressed as 1000 x r^2, where r is equivalent to cosθ (θ = purity angle in Empower).

Similarly, Shimadzu's LabSolutions software uses cosθ values to quantify peak purity. Further, LabSolutions has a built-in feature of "i-PDeA II (Intelligent Peak Deconvolution Analysis II)" to deconvolve coeluted peaks using the algorithm of multivariate curve resolution-alternating least squares (MCR-ALS), the principle of which is discussed further in Section 4.3.3.

Strengths and Weaknesses of PDA-Facilitated UV PPAs

PDA-facilitated PPA, like any analytical technique, has a variety of strengths and weaknesses that should be considered when designing studies in which peak purity data are intended to be used to support conclusions about the stability-indicating capability of the method. Despite its limitations, UV spectral PPA is widely used and well understood in the analytical community within the pharmaceutical industry. It is an efficient and robust means of demonstrating spectral homogeneity of a peak with minimal or no extra cost in terms of time or resources.

One limitation—the potential for false negative results (that is, PPA results exhibiting spectral homogeneity while peaks still contain coeluted compounds)—occurs during spectral peak purity evaluations when:

1. Coeluted impurities have minimal spectral difference.
2. Coeluted impurities have poor UV responses.

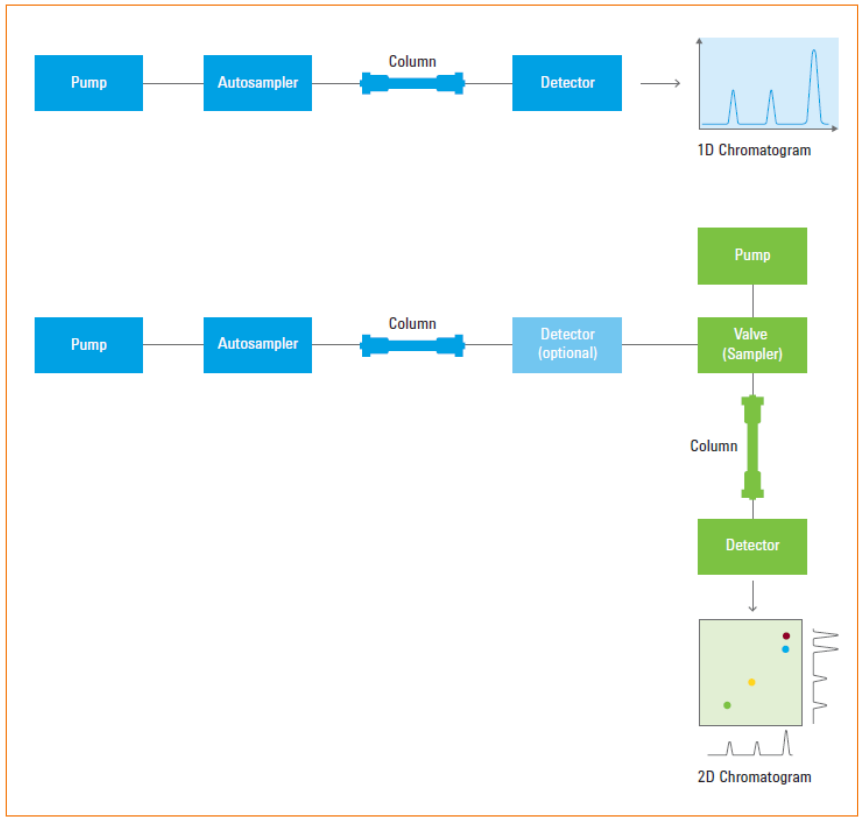

FIGURE 2: High-level comparison of 1D and 2D-LC (reproduced from Figure 1.1 of [18]).

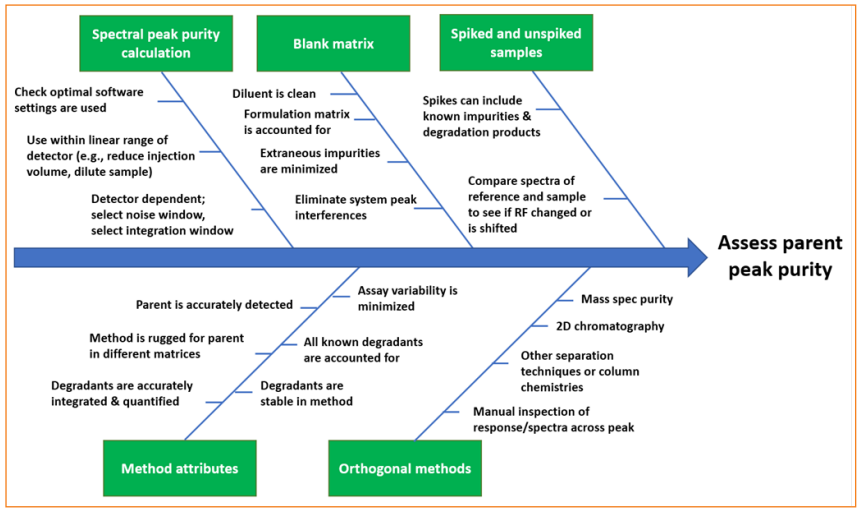

FIGURE 3: Considerations for troubleshooting spectral inhomogeneity.

3. Impurity peaks are eluted near the apex of parent peak.
4. Coeluted impurities are present at very low concentrations.

Similarly, false positives (that is, PPA indicating spectral inhomogeneity for a pure peak) are possible when:

1. There are significant baseline shifts attributable to mobile phase gradients.
2. PPA data processing settings are suboptimal.
3. Integrations are suboptimal, leading to interference from background noise or neighboring peaks at the peak front or tail.
4. UV absorbance measurements are conducted at extreme wavelengths (<210 nm or >800 nm).
5. Impurities are evaluated at low concentrations (<0.1%), making interference from background noise is more pronounced.
6. Artifacts, spurious spikes, and signal-dependent noise appear.
7. Signals are present that are attributable to excipients or other substances unrelated to the API (that is, substances that are not degradants or process-related impurities).

Although they have their limitations, UV spectral PPAs are useful during chromatographic method development and forced degradation studies to confirm separation of the parent analytes from potential degradation products as determined by company best practices. Peak purity determination is not error-proof, and close attention should be paid, especially to borderline circumstances where false negative and positive results may occur.

Mass Spectrometry-Facilitated PPA

PPA by mass spectrometry (MS) is another option used to demonstrate method selectivity and is usually performed by nominal mass resolution single quadrupole mass spectrometers, such as the Waters QDa/SQD or Agilent MSD detectors. The PPA of a compound can be verified by demonstrating that the presence of the same precursor ions, product ions, and/or adducts across the peak that are attributed to the parent compound in the total ion chromatogram (TIC) or extracted ion chromatogram (EIC/XIC) (13).

Different MS instruments and data systems provide varied approaches to estimate mass spectral peak purity.

- On the Waters QDa, the mass spectra extracted at peak front, apex, and tail are compared and examined (14). Obtaining consistent mass spectra at three or

WITH LUMA™ FROM VUV ANALYTICS

Trace Analysis Has Never Been Easier

Introducing a first-of-its-kind, multichannel Vacuum Ultraviolet detector that will shed new light on your Gas Chromatography analysis.

SENSITIVE
to low part per billions (PPB) levels.

SELECTIVE
Acquire up to 12 independent channels of data across a wide wavelength range.

SIMPLE
Fits into existing laboratory workflows and requires minimal training.

UNIVERSAL
Nearly every compound absorbs except for GC carrier gases.

To learn more about how LUMA can shed a new light on your GC analysis, visit:
luma.vuvanalytics.com

VUV ANALYTICS

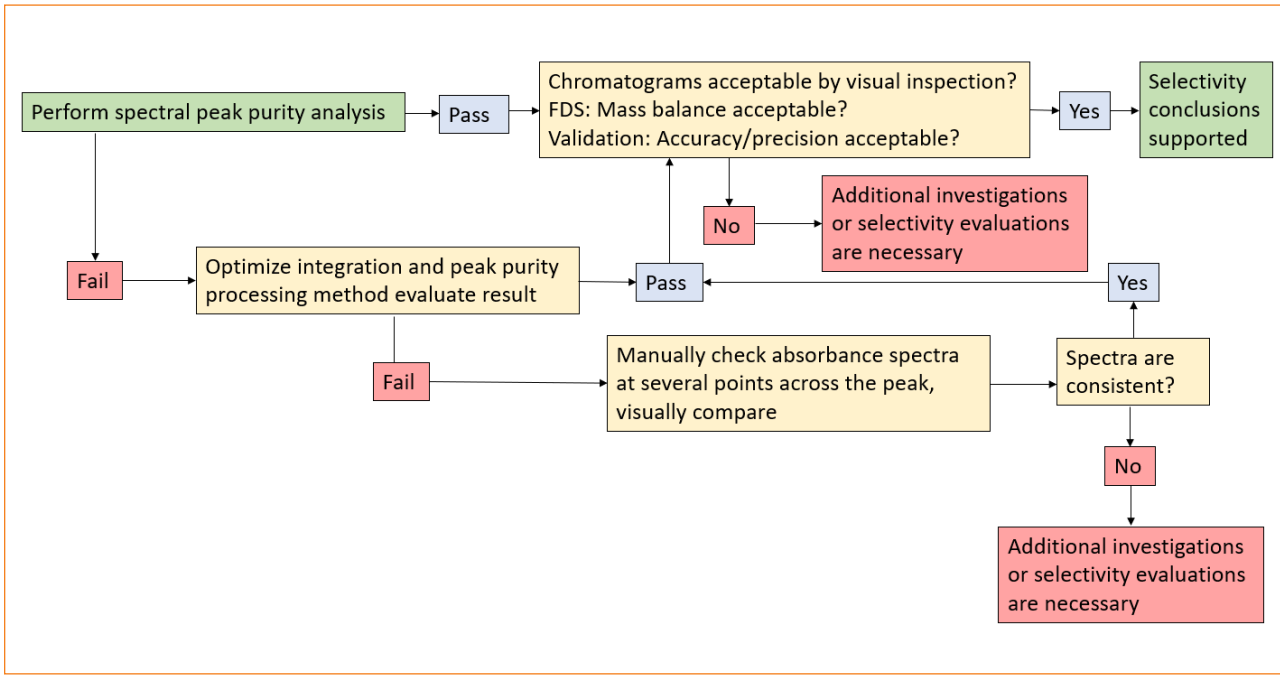

FIGURE 4: PDA (UV) PPA suggested decision tree for determining whether additional investigation by other techniques is necessary for establishing peak purity.

more points across the parent peak provides evidence of peak purity.

- MS peak purity by Agilent MSD is determined by overlaying all the deconvoluted EIC peaks extracted from the TIC of the parent molecule (API) to estimate a MS purity score. A higher score than the configurable passing threshold, or minimum MS purity, suggests adequate peak purity.

The PPA thresholds (that is, the extraction point for the Waters QDa and the relative abundance cut-off for the Agilent MSD) need to be carefully selected to avoid false positives or negatives. The parent compound or impurities might be suppressed or fail to ionize, and impurities can have identical mass-to-charge (*m/z*) ratios as the parent, hindering direct MS determination and increasing the likelihood of false positives or negatives. Excessively high threshold values increase the risk of a false negative (incorrectly passing) PPA as potentially relevant signals may be excluded. Inversely, needlessly low threshold values raise the risk of a false positive (incorrectly failing) PPA because of the inclusion of signals attributable to solvent artifacts, baseline noise, or other responses unrelated to the parent compound, degradants, or process-related impurities. The appropriate threshold value should be determined on a case-by-case basis and varies between experiments, necessitating consideration of the instrumentation (such as cleanliness of the source or the sensitivity of the detector), the selectivity, sensitivity, and robustness of the analytical method, sample ionization efficiency or potential ion suppression, or interference from reagents or excipients, among other factors. It may be beneficial for the selection of the threshold to be accompanied by justification of the decision.

In addition to conducting PPAs with a nominal mass spectrometer, high-resolution MS (HRMS) can also be employed for this purpose. Although these advanced techniques typically require more sophisticated MS equipment (instruments with superior sensitivity, resolving power, and the ability to measure accurate mass) and greater expertise to interpret results, HRMS PPA provides additional evidence on spectral homogeneity by distinguishing masses that are attributed to the compound of interest from those that are not. For example, when acquiring mass spectra using ion trap MS or orbital trap (Tribrid) MS, mass traces are extracted for each peak of interest in TIC by manually selecting and extracting the associated mass spectral data above the peak width of the main component. These extracted mass traces are then overlaid to visually evaluate their congruence, where alignment between the traces indicates the purity of the peak. A detailed analysis of the mass spectra is conducted to determine if all detected masses can be attributed solely to the main component, comparing the observed masses with the expected masses based on the analyte's molecular formula or known impurities.

This evaluation confirms peak purity and identifies any potential coeluted components. Ion trap MS software (Analyst, ProteoWizard) generates a peak list table with relative intensities assigned to detected masses, allowing further analysis of other *m/z* ratios in descending order relative to the intensity of the main mass, providing additional insights into peak purity. The results from such mass spectral PPAs provide further valid evidence of peak purity even in the circumstances when UV spectral PPA information are not available or obtainable.

However, it is important to note that, when using a HRMS instrument, the ratio of attributable to non-attributable masses does not always offer an exact measure of spectral homogeneity. This is primarily because of the challenges in accurately estimating the co-eluting impurity's proportion in the absence of impurity identification and the incorporation of a relative response factor or quantitation via an external standard in most cases. These complexities are attributed to various factors that influence signal response, such as ionization efficiency and signal suppression, for which specific values are not known. Consequently, establishing precise criteria for HRMS PPA becomes challenging because of the need to make various assumptions, including assuming uniform ionization efficiency and consistent response (that is, a relative response factor of one) for all detected compounds.

In essence, although MS PPA does not provide specific values to set acceptance criteria, such as the purity threshold and angle values shown in Table I for PDA assessments, it is advisable to supplement the regulatory submission dossier with more comprehensive explanatory information when conducting this assessment, which will help streamline the data review process.

Additional PPA Methodologies

Orthogonal Chromatographic Conditions

In certain circumstances, such as when the UV spectral PPA are not obtainable (when a PDA detector is not available or when an analyte has poor UV absorbance), peak purity can also be evaluated by employing orthogonal chromatographic conditions, which involve using different stationary phas-

es, such as reversed phases compared to HILIC, or varying the composition of the mobile phase (altering the pH or organic modifiers). These alterations provide orthogonal separation mechanisms. By varying chromatographic conditions and parameters, impurity peaks that might coelute with the parent compound on one system have the potential to be resolved on another, allowing for a more accurate PPA. Moreover, the peak purity can be further investigated by collecting a fraction of the parent peak to be re-analyzed under orthogonal conditions (that is, manual 2D-LC).

2D-LC

Generally, 2D-LC instrumentation is not widely available in many laboratories because it is not a technology typically used for quality control (QC) testing and requires subject matter experts (SMEs) for maintenance and operation. When available, however, one of the most powerful capabilities of this technique is its ability to physically separate components that may be coeluted with the compound of interest under one set of chromatographic conditions.

2D-LC achieves this by subjecting effluent from one chromatographic system to a second set of chromatographic conditions. The combination of two different separation mechanisms results in improved resolution and separation of components in complex samples, where the two sets of conditions are joined through a "heart-cutting" or "fraction collecting" process. This process first separates components under the normal (or nominal) chromatographic conditions (1D), then makes use of a post-column sampling valve that diverts the flow of effluent at the expected retention time(s) of the peak(s) of interest, to the second separative system (2D).

2D-LC may also be used as an alternative method development tool or for investigations in forced degradation studies (15–17). Figure 2 exhibits a high-level illustration of the operation mechanisms of 1D and 2D-LC, permitting comparison of the two approaches (18). Using sequential chromatographic systems with orthogonal conditions or columns expands the separative ability of each system, offering superior overall selectivity that can separate coeluted peaks. Peak purity using this technique can be evaluated by comparing various characteristics, including chromatographic profiles, UV spectra, and mass spectra obtained from different dimensions. Deviations or overlaps in these characteristics may indicate the presence of coeluted components or impurities, suggesting potential purity concerns (17).

PPA by Chemometrics

Chemometric techniques are also used to provide robust analyses using PDA spectral data by deconvoluting peaks composed of major and minor components (15). In principle, these techniques analyze the matrix of absorbance measurements at all wavelengths (that is, spectra) and at all time points across a given time region in the chromatogram. Using a regression-based approach to determine how the spectra change over time, any impurities cannot only be discovered, but also be mathematically resolved from the target peak. Several algorithms for PPA, including principal component analysis (PCA), evolving factor analysis (EFA), and, more recently, multivariate curve resolution-alternating least squares (MCR-ALS) have been reported in literature (19–22). However, these algorithms have neither not been widely implemented in commercial chromatographic data systems, nor have any reports comparing PPA results by chemometrics versus those determined by commercial software been published. As this technology is in its early stages of development, it should be considered an optional, potentially emerging, investigational tool for PPA assessments.

Summary of Current PPA Best Practice

According to the information provided by the contributing analytical chemistry experts who are employed by global pharmaceutical companies, PPA results are typically part of the marketing application FDS data package supporting the suitability of a stability-indicating method. PPAs are performed on the peaks of parent compounds in chromatograms from samples stressed under various conditions to demonstrate confidence that no peaks attributed to degradation products are coeluted with the parent compound, thereby providing supporting information that the method is stability indicating. Typically, forced degradation is allowed to proceed until either 5–20% degradation of the API or drug product is achieved, or the pharmaceutically relevant endpoints of the stress conditions are reached (23,24). Figure 3 shows an Ishikawa (fishbone) diagram exhibiting factors to be considered when assessing the purity of the parent peaks in a method. Along the lines connecting these boxes to the central backbone are example components that provide more detail for each factor. This diagram serves as a troubleshooting tool when investigating why a particular PPA for a given method has indicated spectral inhomogeneity.

Multiple factors should be considered when interpreting the results of parent peak purity assessment. The execution of appropriate FDS conditions to reach target degradation levels or scientifically justified endpoints (24) is essential to obtain meaningful PPA results. In determining the purity of a parent peak, along with obtaining acceptable PPA data, other information such as mass balance and response factors of expected degradants should be assessed to mitigate the risk of false negative results. When PPA results do not meet purity criteria, precautions should also be taken to avoid false positive results

because of inappropriate data processing and interpretation. Figure 4 displays a flow chart that summarizes a suggested approach to interpreting PPA results and the circumstances under which further investigation may be appropriate.

After obtaining evidence that the parent peak in a partially degraded or stressed sample is spectrally impure, assuming the stress condition is pharmaceutically relevant (24) for the API or drug substance (DS) and/or drug product (DP), further investigation to understand the nature and origin of the coeluted species should be considered. Such an investigation may include assessments of known impurities and/or excipients, orthogonal detection techniques, and/or orthogonal methods such as 2D-LC. Ultimately, it may be necessary to redevelop the analytical method to ensure the method is stability indicating. However, if suitable justification can be provided (such as evidence that the coeluted impurity is not relevant to long-term stability), redevelopment of the method may not be required. These types of circumstances should be addressed on a case-by-case basis using sound scientific reasoning and approaches.

Final Recommendations to Guide PPA

It is recommended that PPA be performed as part of a FDS using the commercial software as a part of stability-indicating method development and validation activities that support regulatory submissions (that is, marketing applications) of pharmaceutical data. Software-calculated spectral PPAs are widely used in the analytical community within the pharmaceutical industry. In FDSs, such PPA techniques are an efficient and robust means to demonstrate spectral homogeneity of the parent peaks in stressed DS or DP sample chromatograms.

PPAs facilitated by PDA detection are most used and are applicable to most small molecule APIs. Under the circumstances when UV spectral PPA information are unavailable or unobtainable, PPA results obtained by other techniques, such as MS, are equally valid provided that appropriate peak purity criteria are met. Questionable or aberrant PPA data, including false negative or positive results, may be obtained in borderline circumstances or due to suboptimal data processing and result interpretation.

Because of these limitations, a PPA cannot prove unequivocally that a peak is pure; a PPA can only conclude that no coeluted compounds were detected. However, potential selectivity issues of a stability-indicating method should not be evaluated with peak purity results alone. Indeed, PPA issues often coincide with other readily observable analytical and chromatographic concerns such as poor mass balance, poor resolution and column efficiency, or matrix interference. As such, other chromatographic elements that affect method selectivity should be evaluated in conjunction with PPA, even when PPA result acceptance criteria are met. If the data indicate that the parent peak is spectrally impure, orthogonal detection, orthogonal methods, and/or 2D-LC are potential supplementary options for further investigation.

The authors hope that this review serves a useful overview and resource for analytical scientists, both inside and outside the pharmaceutical industry, as well as for associated pharmaceutical HA representatives and reviewers.

Disclaimer

Employers of the authors of this article, and any other companies noted herein, did not contribute to this article or any of the articles referenced, nor did they provide funding support for any part of this paper. Contributions by authors are limited to time spent writing, editing, performing literature research, discussing, and sharing expert insights gleaned over the course of their respective careers.

Acknowledgement

The authors gratefully acknowledge the following individuals for their technical assistance and support: Paul Gerst, Scott Jennings, and Flavia Firmino. ■

This article has additional supplemental information only available online.
Scan code for link.

ABOUT THE AUTHORS

Pascal Marillier and **Neal Adams** are with Scientific and Laboratory Services – Analytical Sciences at Pfizer Inc, in Kalamazoo, MI.

Steven W. Baertschi is with Baertschi Consulting LLC, in Carmel, Indiana.

John M. Campbell is with Analytical Development at GkaxoSmithKline, in Upper Providence, PA.

Chris Foti and **Liping Meng** are with Analytical Development and Operations at Gilead Sciences Inc., in Foster City, CA.

Juçara Ribeiro Franca is with the Brazilian Health Regulatory Agency (ANVISA), in Brasilia, Brazil.

Simon Hicks is with Analytical Development, at GlaxoSmithKline in Stevenage, UK.

Dorina Kotoni is with Chemical & Analytical Development at Novartis Pharma AG, in Basel, Switzerland.

Christian Laue is with Chemical & Pharmaceutical Development at Merck Healthcare KGaA, in Darmstadt, Germany.

Stacey Marden is with Advanced Drug Delivery, Pharmaceutical Sciences, R&D, at AstraZeneca, in Boston, MA.

Ana Claudia de Oliveira Santos is with Global Analytical Technology at Merck Brazil, in São Paulo, Brazil.

Mariah Ultramari is with Spektra Soluções Científico-Regulatórias Ltda, in São Paulo, Brazil.

An Van Cleempoel is with Small Molecule Method Development at Janssen Pharmaceutica, Johnson & Johnson, in Beerse, Belgium.

Chloe Wang is with Analytical Development at Jazz Pharmaceutical, in Palo Alto, CA.

Todd Zelesky is with Analytical Research & Development at Pfizer Inc., in Groton, CT.

Zongyun Huang is with Drug Product Development at Bristol-Myers Squibb Co., in New Brunswick, NJ.

Direct correspondence to Zongyun Huang at **zongyun.huang@bms.com**

A Flash Qualitative Identification Method for the Specific Component in a Mixture Based on Diode Array Detector

Lizhi Cui, Xuan Li, Zebin He, Yi Yang, Bingfeng Li, Keping Wang, Xinwei Li, Junqi Yang, Xuhui Bu, and Weina He

This paper proposes a new method of flash qualitative identification (FQI) to qualitatively identify a certain target component from a mixture within half a second by disusing the analytical column, which is a time-consuming unit in current chromatography instruments. First, a Noised Spectrum Identification (NSI) model was constructed for the data set generated directly by diode array detector (DAD) without the process in an analytical column. Then, a method called vector error algorithm (VEA) was proposed to generate an error according to the DAD data set for a mixture and a specific spectrum for the target component to be identified. A criterion based on the error generated by the VEA is used to give a judgement of whether the specific spectrum exists in the DAD data set. Several simulations demonstrate the high performance of the FQI method, and an experiment for three known materials was carried out to validate the effectiveness of this method. The results show that the NSI model concurs with the real experiment result; therefore, the error generated by the VEA was an effective criterion to identify a specific component qualitatively, and the FQI method could finish the identification task within half a second.

CHROMATOGRAPHY has been developed as a set of laboratory techniques that are widely applied in the quality control (QC) of mixtures such as herbal medicine, grape wine, petroleum, judicial expertise, and others. Chromatography is further classified as gas chromatography (GC) and liquid chromatography (LC) according to the mobile phase. With the development of the modern instrument, the ultrahigh-pressure LC (UHPLC) technique was born. High performance liquid chromatography (HPLC) is an important branch of chromatography. HPLC uses liquid as the mobile phase, and it employs a high-pressure infusion system to pump a single solvent with different polarities, or mixed solvents and buffers, in different proportions into the stationary phase. After the components in the column are separated, the chromatographic column enters the detector for detection to realize the analysis of the sample. Compared with HPLC, UHPLC has the advantages of higher resolution, faster speed, and greater sensitivity. Although the technique improves the speed, sensitivity, and resolution of HPLC, its original practicability and principle are retained. The significant advantage of UHPLC is that it can shorten the analysis time and improve work efficiency (for example, for a related substance analysis method, the use of HPLC to run a needle is 75 min; with UHPLC, this task can be completed in 10 min), and the analysis efficiency is increased by nearly 7.5 times. Of course, the analysis efficiency has been improved so much that the supporting equipment is certainly not for fun. UHPLC requires a small particle hybrid packing (1.7 µm) column, a higher pressure (up to 15000 psi), and a low system volume infusion unit. Although the supporting equipment can greatly shorten the analysis time depending on the complexity of the sample, it usually takes many minutes to complete the analysis process. To reduce the time consumed during the process

of the chromatography, the diode array detector (DAD), combined with chemometrics methods such as evolving factor analysis (EFA) (1–3), multivariate curve resolution alternating least square (MCR-ALS) (4–7), the iterative algorithm (IA) (8,9), independent component analysis (ICA) (10,11), general reference curve measurement (GRCM) (12,13), and more, are introduced to pick chromatogram peaks from the raw data set generated by the hyphenated instrument of HPLC and DAD (14). The above methods could improve the resolution of the instruments, but they cannot reduce the time consumed during the chromatography process because it is influenced by the analytical column.

As shown in Figure 1, the analytical column is the time-consuming unit in a HPLC (or UHPLC) instrument. To further cut down the time used for an analysis process, this paper proposes a totally new software calculation method to qualitatively identify a specific component from a mixture within half second by disusing the analytical column. Because this method reduces the time for analysis sharply from 10–30 min down to around 200 ms, we call it the *flash qualitative identification (FQI)* method. Furthermore, the remove of the analytical column will reduce the requirement of the high-pressure pump.

The remainder of this paper is arranged as follows: the principle of the FQI Method is introduced; the simulations and experiments to demonstrate the performance and practicability of this method are provided; and then we draw the conclusions from our study and propose future works.

The FQI Method

The operation process of the FQI method is demonstrated in Figure 2. First, the objective material for analysis is prepared to be a sample. Then, input the sample into the instrument to generate DAD data set D. On the other hand, the spectrum c^* of the specific component to be identified is abstracted from the standard database. When the DAD data set D and the spectrum c^* is inputted into the vector error algorithm (VEA), an error ε will be generated. Finally, the result of positive or negative could be given

based on the error ε. The modeling for the DAD data set is introduced first; then, the design of the VEA will be explained carefully based on the DAD model.

Modelling for DAD Data Set

For component analysis, the model for HPLC-DAD data set as shown in equation 1 was used widely in many references (15,16)

$$x_{w\times t} = \sum_{i=1}^{n} a_i \times s_i^t + n = [a_1, a_2, \cdots, a_n] \times \begin{bmatrix} s_1 \\ s_2 \\ \vdots \\ s_m \end{bmatrix} = a \times s + \tilde{n} \quad [1]$$

where X is the HPLC-DAD data set with the dimension of $w \times t$. The dimension w represents the wavelength, and the dimension t represents the sampling point along the retention time. a_i, $i = 1,2,\cdots, n$ are the column vectors indicating all the individual spectra. s_i^t, $i = 1,2,\cdots, n$ are the row vectors indicating all the chromatogram peaks. The digital n is the number of the components contained in the data set X. The matrix N is the Gaussian noise. However, the model shown in equation 1 is not suitable for the research in this paper for the following two reasons, which are explained based on a simulated sample containing four components as shown in Figure 3.

The first reason is because of the effect of the analytical column, the chromatographic peaks for different components express various values in width and peak position as shown in Figure 3a. Theoretically speaking, this feature makes the data set $X = [a_1,a_2,a_3,a_4] \times [s_1,s_2,s_3,s_4]^T$, shown in Figure 3c, with the rank of four. However, if the analytical column was removed from the experimental system, the chromatographic peaks for all the components would share the same width and peak position as shown in Figure 3d according to the principle of the chromatography, which means the data set generated by $X_1 = [a_1',a_2',a_3',a_4'] \times [s_1,s_2,s_3,s_4]^T$, has the rank of one. Currently, there is no method could pick from a_1' or s_1 from X_1. In Figure 3, the axis of *mAu* is the signal strength.

The algorithm proposed in our previous works based on equation 1 is to peak chromatogram peaks from s_i from X, and then to calculate spectra a_i based on s_i and X. In this paper, what we want to finish is to find a

flash qualitative identification method for a specific component based on its spectrum. Therefore, the model shown in equation 1 is not suitable.

Based on the analysis above, the following noised spectrum identification (NSI) model is proposed.

$$\begin{cases} \mathrm{d}_{t\times w} = \sum_{i=1}^{n} \mathrm{d}_i = \sum_{i=1}^{n} \mathrm{p}_i \times \mathrm{c}_i^t = [\mathrm{p}_1, \mathrm{p}_2, \cdots, \mathrm{p}_n] \times \begin{bmatrix} \mathrm{c}_1^t \\ \mathrm{c}_2^t \\ \vdots \\ \mathrm{c}_n^t \end{bmatrix} = \mathrm{p} \times \mathrm{c} \\ \mathrm{p}_i = \bullet_i(\mathrm{p}) \end{cases} \quad [2]$$

where D is the DAD data set with the dimension of $t \times w$. The dimension t represents the sampling point along the process time, and the dimension w represents the wavelength. p_i, $i = 1,2,\cdots$, n are the column vectors indicating all individual chromatogram peaks. The vector p is a single peak curve to express the process for the mixture passing through the DAD instrument. c_1^t, $i = 1,2,\cdots$, n are the row vectors indicating all the spectra. The digital n is the number of the components contained in the data set D. The function $\bullet_i(p)$ adds different Gaussian noise to the vector p to generated vectors p_i.

The Design of VEA

Based the DAD model shown in equation 2 and the principle shown in Figure 2, following objective function is given.

$$\begin{cases} \min\ \{\|\mathrm{y}^t - \mathrm{c}^{*t}\|_2^2\} = \min\ \{\varepsilon\} \\ \mathrm{y}^t = \mathrm{w}^t \times \mathrm{d} \rightarrow \mathrm{c}^{*t} \end{cases} \quad [3]$$

where the vector w is unknown to construct vector y; the vector c^* is the spectrum of the component which is going to be identified; the scalar of ε is the error between y and c^*; the operator $\|g\|_2^2$ is the 2-norm of a vector; the note $\rightarrow$ means y looks like c^* in shape. To solve equation 3, we rewrite it as

$$\begin{cases} \min\{\|\mathrm{y}^t - \mathrm{c}^{*t}\|_2^2 = \|\mathrm{w}^t \times \bar{\mathrm{d}} + \mathrm{w}^t \times \mathrm{m}^{-1} \times \tilde{\mathrm{d}} - \mathrm{c}^{*t}\|_2^2\} \\ \mathrm{d} = \begin{bmatrix} \mathrm{d}_{t1} \\ \mathrm{d}_{t2} \\ \vdots \\ \mathrm{d}_{tt} \end{bmatrix} = \mathrm{d} + \tilde{\mathrm{d}} = \begin{bmatrix} \bar{\mathrm{d}}_{t1} \\ \bar{\mathrm{d}}_{t2} \\ \vdots \\ \bar{\mathrm{d}}_{tt} \end{bmatrix} + \begin{bmatrix} \tilde{\mathrm{d}}_{t1} \\ \tilde{\mathrm{d}}_{t2} \\ \vdots \\ \tilde{\mathrm{d}}_{tt} \end{bmatrix} \\ \tilde{\mathrm{d}} = [\tilde{\mathrm{d}}_{c1}, \tilde{\mathrm{d}}_{c2}, \cdots \tilde{\mathrm{d}}_{cw}] = \mathrm{m} \times \hat{\mathrm{d}} = \mathrm{m} \times [\tilde{\mathrm{d}}_{c1}, \tilde{\mathrm{d}}_{c2}, \cdots \tilde{\mathrm{d}}_{cw}] \end{cases} \quad [4]$$

where d_{ri}^t, $i = 1,2,\cdots t$ are row vectors of matrix D; d_{ri}^t, $i = 1,2,\cdots t$ are row vectors, whose elements all equal to the mean value of d_{ri}^t, $i = 1,2,\cdots t$; d_{ri}^t, $i = 1,2,\cdots t$ are row vectors after removing mean value from d_{ri}^t, $i = 1,2,\cdots t$; the matrix D is transformed from the matrix D by a linear transformation, which makes the column vectors d_{ci}^t, $i = 1,2,\cdots w$ not correlated from each other and normalized as shown in equation 5. The method to obtain the matrix M is introduced in Appendix A.

$$e\{\tilde{\mathrm{d}}_{ci} \times \tilde{\mathrm{d}}_{ci}^t\} = \mathrm{i}_{t\times t} \text{ or } e\{\tilde{\mathrm{d}} \times \tilde{\mathrm{d}}^t\} = w \times \mathrm{i}_{t\times t} \quad [5]$$

After analyzing equation 4, the term of $w^T \times \bar{\mathrm{d}}$ equals to a constant vector, so equation 4 is reconstructed as

$$\begin{cases} \min\{\|\bar{\mathrm{b}}^t \times \tilde{\mathrm{d}}^* - \mathrm{c}^{*t}\|_2^2\} \\ \bar{\mathrm{b}}^t = [\mathrm{b}^t, d] \\ \tilde{\mathrm{d}}^* = \begin{bmatrix} \tilde{\mathrm{d}} \\ 1 \end{bmatrix} = \begin{bmatrix} \tilde{\mathrm{d}}_{c1} & \tilde{\mathrm{d}}_{c2} & \cdots & \tilde{\mathrm{d}}_{cw} \\ 1 & 1 & \cdots & 1 \end{bmatrix} = [\tilde{\mathrm{d}}_{c1} \ \ \tilde{\mathrm{d}}_{c2} \ \ \cdots \ \ \tilde{\mathrm{d}}_{cw}] \\ e\{\tilde{\mathrm{d}}^* \times \tilde{\mathrm{d}}^{*t}\} = w \times \mathrm{i}_{(t+1)\times(t+1)} \end{cases} \quad [6]$$

where d is a constant, and w is the number of the wavelength. Appendix B gives the reason why $e\{\tilde{\mathrm{d}}^* \times \tilde{\mathrm{d}}^{*t}\} = w \times \mathrm{i}_{(t+1)\times(t+1)}$. According to Karush-Kuhn-Tucher condition (17), the solution of equation 6 satisfies

$$f(\bar{\mathrm{b}}^t) = \sum_{j=1}^{w} 2 \times \tilde{\mathrm{d}}_{cj}^{*t} \times (\bar{\mathrm{b}}^t \times \tilde{\mathrm{d}}_{cj}^* - \mathrm{c}^{*t}(j)) = 0 \quad [7]$$

where c^{*T} is the jth element in the vector c^{*T}. The Newton method (18) is adopted to solve equation 7, whose Jacobian matrix is calculated as

$$jf(\bar{\mathrm{b}}^t) = \sum_{j=1}^{w} 2 \times \tilde{\mathrm{d}}_{cj}^* \times \tilde{\mathrm{d}}_{cj}^{*t} \quad [8]$$

Then, the iteration for $\bar{\mathrm{b}}^t$. can be given as

$$\bar{\mathrm{b}}^* = \bar{\mathrm{b}} - \frac{\sum_{j=1}^{w} 2 \times \tilde{\mathrm{d}}_{cj}^* \times (\bar{\mathrm{b}}^* \times \tilde{\mathrm{d}}_{cj}^* - \mathrm{c}^{*t}(j))}{\sum_{j=1}^{w} 2 \times \tilde{\mathrm{d}}_{cj}^* \times \tilde{\mathrm{d}}_{cj}^*} = \frac{\sum_{j=1}^{w} \tilde{\mathrm{d}}_{cj}^* \times \mathrm{c}^{*t}(j)}{w \times \mathrm{i}} = \frac{1}{w} \times \tilde{\mathrm{d}}^* \times \mathrm{c}^{*t}(j) \quad [9]$$

Consequently, the curve of y^T can be calculated by following equation.

$$\mathrm{y}^t = \bar{\mathrm{b}}^t \times \tilde{\mathrm{d}}^* = \mathrm{c}^{*t} \times \left(\frac{1}{w} \times \tilde{\mathrm{d}}^{*t} \times \tilde{\mathrm{d}}^* \right) \quad [10]$$

Finally, the judgment for whether a specific component is contained in a mixture could be given by the criterion as shown in equation 11.

$$\begin{cases} \text{Positive}, \varepsilon = \|\mathrm{y} - \mathrm{c}^*\|_2^2 < \varepsilon^* \\ \text{Negative}, \varepsilon = \|\mathrm{y} - \mathrm{c}^*\|_2^2 \geq \varepsilon^* \end{cases} \quad [11]$$

where the scalar value of ε^* is a presetting small digital. Equation 3 is called the VEA. The scalar of ε is the output of VEA. Equation 11 is the criteria equation based on the VEA.

Simulations and Experiments

In this section, a group of simulations demonstrate the performance of the FQI method. On this basis, the minimum range of difference between target spectra and nontarget spectra is proved. Then, a data set, generated from HPLC-DAD instrument without passing through the analytical column, is calculated by the FQI method to indicate its effectiveness.

Simulations and Discussions

The simulation data set was generated by equation 2, where n is set to six. The vectors a_1' shown in Figure 3d mixed with different level of Gaussian noise were selected as p_1 in equation 2. The vectors s_1 shown in Figure 3b mixed with different levels of Gaussian noise were selected as c_1 in equation 2.

For this study, 20 simulation data sets with different noise levels (SNR = 200, ..., 30, 20, 10, 1) are generated equation 2. Four simulation data sets (SNR = 40, 20, 10, 1) are listed in this paper. As shown in Figure 4, 18 spectra curves are calculated by the FQI method, among which $s_{1\text{-}4}$ are known spectra contained in the data set D, and $s_{5\text{-}18}$ are spectra constructed different from $s_{1\text{-}4}$ in shape. The errors ε given by equation 3 for $s_{1\text{-}18}$ are listed in Table I.

Among the 18 spectral curves, s_1 was selected as the experimental analysis object. As shown in Figure

5a, the eight curves changed in varying degrees on the basis of $s_1 \cdot s_1^2$ is the overall offset of one unit on the basis of s_1, and s_1^3 is the overall offset of two units on the basis of $s_1 \cdot s_1^4 - s_1^9$ is to change one of the 100 pixel points. Figure 5b is a graph of five distance formulas and corresponding errors for Euclidean distance, Mahalanobis distance, Chebyshev distance, chi-square distance, and Hamming distance. Among them, the red curve is Euclidean distance, Mahalanobis distance, and Chebyshev distance, these three curves coincide. Blue is chi-square distance and green is Hamming distance. We choose the Euclidean distance according to the experimental results. Table II lists the errors ε corresponding to the Euclidean distance of the nine deviation curve in Figure 5a. From the results, we can see:

- The error ε calculated by the VEA is an effective criterion for judging whether a specific spectrum exists in the mixture and judge the similarity between them. In Table I, no matter how serious the noise existing in the data set is, the errors for the spectra of $s_{1\text{-}4}$ are always significantly smaller than those for $s_{5\text{-}18}$, which are different from $s_{1\text{-}4}$ in shape.
- Although four simulation data sets are generated by different noise levels, the final error results are almost the same. It can be seen from Table I that although the error of $s_{1\text{-}4}$ fluctuates, the error of $s_{5\text{-}18}$ does not change, which shows the experimental results are little affected by noise.
- The error ε calculated by the VEA is stable regardless of the noise level in the data set. In Table I, all errors calculated for $s_{5\text{-}18}$ are always the same although the noise levels are different. The differences among the errors for $s_{1\text{-}4}$ under various noise level may be caused by the calculation error of the computer.
- As can be seen from Table II, the greater the deviation distance, the greater the error. Our study found that the spectral curve allowed 0.3 offset distance. When $\Delta < 0.3$, it is shown that the curve exists in the mixture, and when $\Delta > 0.3$, the curve does not exist in the mixture.

Experiments and Discussions

The reference materials of $C_6H_4SO_2NNaCO \cdot 2H_2O$ (GBW (E) 100008, 1.00 mg/mL), $C_4H_4KNO_4S$ (GBW (E) 1001711.00 mg/mL), $C_6H_8O_2$ (GBW (E) 100007, 1.00 mg/mL) were purchased from the National Institute of Metrology in China. Then, 0.5 mL of

the abovementioned three materials were abstracted separately and mixed with water until the mixture had a volume of 10 mL. The chromatography instrument used was provided by Waters and equipped with a 2695 separating element, a 2998 DAD, and an Empower 3 workstation. The scan model is 3D with wavelength from 200 nm to 500 nm. The flow rate is set at 0.5 mL/min. The amount of the sample is selected as 10 µL.

Four DAD data sets of D, D_1, D_2, D_3 are generated by the instrument without the analytical column for the mixture, the $C_6H_4SO_2NNaCO \cdot 2H_2O$, the $C_4H_4KNO_4S$, and the $C_6H_8O_2$ respectively. The time used for the individual experiment is only 0.2 second. And three spectra of $s_{1\text{-}3}$ can be abstracted for the three materials from D_1, D_2, D_3 in Figure 6. Similarly as the simulations, thirteen spectra of $s_{4\text{-}16}$, shown in Figure 7, are constructed based on $s_{1\text{-}3}$, which are different from $s_{1\text{-}3}$ in shape. We input the matrix D and the spectra $s_{1\text{-}16}$ into the VEA, the errors are shown in Figure 8 and Table III.

Similar to the simulation experiment, we selected s_3 as the experimental analysis object in these 16 spectral curves. As shown in Figure 9a, s_3^2 is the overall offset of one unit on the basis of s_3, and s_3^3 is the overall offset of two units on the basis of s_3 • s_3^4 - s_3^9 is to change one of the 244 pixel points. Figure 9b is a graph of the errors corresponding to the five deviation distances. Table IV lists the errors ε corresponding to the euclidean distance Δ of the nine deviation curve in Figure 9a. From the results, we can see:

- The error calculated by the VEA could be used as a criterion to judge whether the mixture contain specific material represented by its spectrum. The size of the error is inversely proportional to whether the mixture contains the specific material represented by its spectrum. When the error is small enough or tends to be stable, it can be said that the mixture contains the specific material represented.
- It can be seen from Figures 7 and 8 that the errors for $s_{1\text{-}3}$ are smaller than those for $s_{4\text{-}16}$. The reason why the errors for s_{10} and s_{12} are close to those for $s_{1\text{-}3}$ is because the shape of s_{10} and s_{12} are close to the shape of s_2. However, the error of s_6 is the biggest because the shape difference between s_6 and $s_{1\text{-}3}$ is the biggest. This error shows that it is necessary to construct the curve according to the shape of the spectrum, and the similarity between the curve and the real spectrum determines its accurate value.
- The larger the amount of the material, the smaller the error calculated for its spectrum. In Table III, the error for s_2 is much smaller than those for s_1 and s_3. The reason could be that the amount of the material represented by s_2 is larger than those represented by s_1 and s_3. From Figure 7, the amplitude of s_2 is obviously bigger than those for s_1 and s_3.

Conclusions and Future Work

Conclusions

- A mathematical model named NSI for DAD data set was proposed in this paper. And based on this NSI model, a FQI method was proposed to identify a specific material from a mixture within half second. Through simulations and experiments, the method was proved to be effective and efficient in the qualitative identification for a specific material from a mixture.
- The gap between the errors given by the VEA for target spectra, such as $s_{1\text{-}4}$ in Figure 4, and non-target spectra, such as $s_{5\text{-}18}$ in Figure 4, is significant for simulations, whereas this gap for experiments is much smaller but still could be used as a criterion to finish the qualitative identification.
- The FQI method proposed in this paper did not need the analytical column in the instrument, and could finish the identification within half second. This feature would bring a big change in the analytical research.

Future Work

- For experiments, how to enlarge the gap between errors for target spectra and non-target spectra will be researched in the near future, which will make the method more practical.
- For some application, the qualitative identification is not enough, so relative quantitative analytical method based on the FQI method should be proposed in the future, which could enhance the practicability of this method.

Acknowledgment

This work was supported in part by National Natural Science Foundation of China under Grant 61973105, Henan Natural Science Foundation under Grant 162300410125, Innovative Scientists and Technicians Team of Henan Provincial High Education (20IRTSTHN019), the Innovative Scientists and Technicians Team of Henan Polytechnic University (T2019-2), and the Henan Polytechnic University Doc Fund under Grant B2016-16. ■

This article has additional supplemental information only available online.
Scan code for link.

ABOUT THE AUTHORS

Lizhi Cui, Xuan Li, Zebin He, Yi Yang, Bingfeng Li, Keping Wang, Xinwei Li, Junqi Yang, and **Xuhui Bu** is with the School of Electrical Engineering and Automation at Henan Polytechnic University, in Henan, China.

Weina He is with the School of Computer at Pingdingshan University, in Henan, Pingdingshan, China.

Direct correspondence to Xuan Li at **lixuan592021@163.com**

UHPLC HILIC Columns

iHILIC®-Fusion and iHILIC®-Fusion(+) have two lines of 1.8 µm UHPLC HILIC columns with different surface chemistries. They provide customized and complementary selectivity, ultimate separation efficiency, and ultra-low column bleeding. The columns are particularly suitable for LC-MS based applications in the analysis of polar compounds.

HILICON AB
info@hilicon.com | www.hilicon.com
Tvistevägen 48 A, SE-90736 Umeå, Sweden

HiSorb™ – High-capacity sorptive extraction

HiSorb™ – high-capacity sorptive extraction – is a labour-saving and cost-effective sampling technique for the analysis of trace-level (S)VOCs in liquids and solids. Used with thermal desorption–GC–MS, HiSorb is suitable for both headspace and immersive sampling. Detection limits are lower than with other techniques, such as SPME, because of the large capacity of sorptive phase. HiSorb probes come in multiple phases for a wide range of applications, and the technique is easier and quicker to use than solvent extraction. Re-usable probes and tubes minimise the cost per sample, and are robust and easy-to-use.

Markes International Ltd
enquiries@markes.com | https://chem.markes.com/LCGC/HiSorb
Markes International Ltd., Bridgend, UK

Highly reproducible IEX columns

YMC's BioPro IEX columns are the 1st choice for high resolution analysis of antibodies, proteins, and oligonucleotides with high recovery. BioPro IEX columns are based on non-porous or porous hydrophilic polymer beads with low nonspecific adsorption. Excellent lot-to-lot reproducibility ensures reliable results in analytical and (semi) preparative scale as well as when coupled to MS.

YMC Europe GmbH
support@ymc.eu | https://ymc.eu/iex-columns.html
Schöttmannshof 19, D-46539 Dinslaken, Germany

GC Detector

VICI's Model D-3-1-8890 is a "plug-and-play" pulsed discharge detector for easy installation and configuration on the Agilent 8890 GC. This detector is optimized for trace-level work in helium photoionization mode, and is a non-radioactive, low maintenance universal detector with a wide linear range. It also utilizes the electronics and power supply of the host GC.

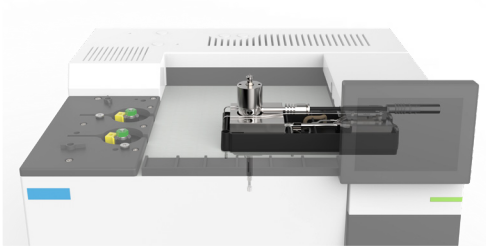

VICI AG International
info@vici.ch | www.vici.com
Parkstrasse 2, CH-6214 Schenkon, Switzerland

Capper

The Ultraseal Cap-Pro is a semi-automated sealing solution that reportedly takes the strain out of applying friction sealing mats and septum sealing caps to microplates and tube racks. Within seconds, this benchtop-friendly capper seals all samples securely for reliable sample handling and storage, according to the company.

Porvair Sciences
int.sales@porvairsciences.com
www.microplates.com/product/ultraseal-cap-pro/
Porvair Sciences, Wrexham, UK

Nitrogen Solution

Genius XE Nitrogen is a cutting-edge evolution combining advanced technology with refined, robust engineering, according to the company. With two models—XE 35 (up to 35 L/min) and XE 70 (up to 70 L/min)—it provides a standalone nitrogen solution for high performance LC–MS/MS and other mission-critical laboratory applications.

Peak Scientific
www.peakscientific.com
Peak Scientific, Inchinnan, Scotland.

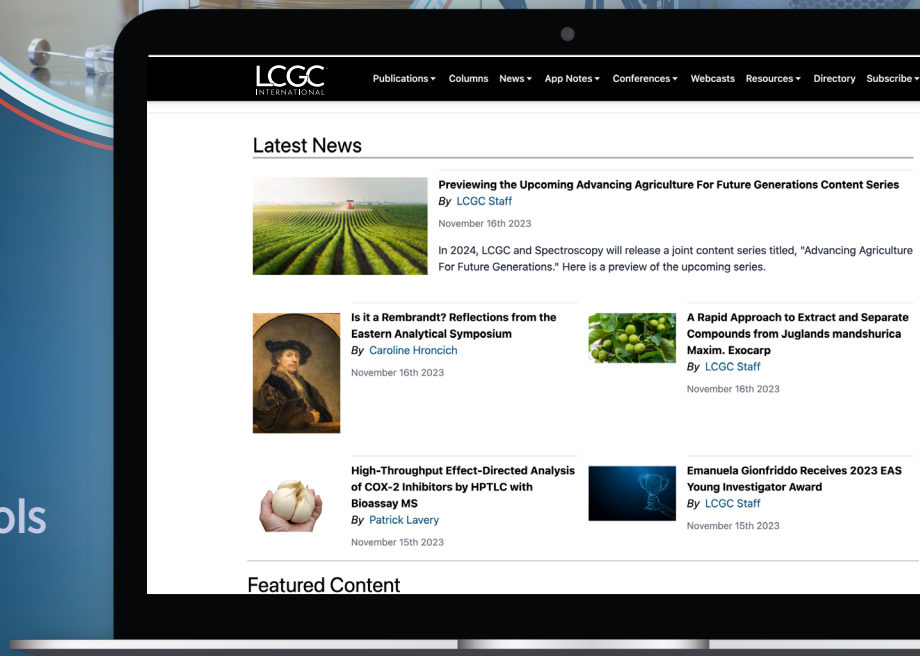

Online Learning

Visit our website for the latest online learning tools for chromatographers!

- Webcasts
- Digital Publications
- eBooks
- Application Notes
- Videos
- News Updates
- Industry Insights
- And more!

LCGC™ INTERNATIONAL

Visit us at: ChromatographyOnline.com

Syft™

Syft Tracer Pharm11

The only compliant real-time mass spec for Pharma / CDMO Applications

A complete solution for high-throughput, 21 CFR Part 11 compliant, automated workflows

Debuting **Worldwide**

Schedule Your **Live** Demo

Learn More

www.syft.com